

TRANSFORMERS AS INTRINSIC OPTIMIZERS: FORWARD INFERENCE THROUGH THE ENERGY PRINCIPLE

Ruifeng Ren, Sheng Ouyang, Huayi Tang, Yong Liu*

Gaoling School of Artificial Intelligence,

Renmin University of China

{renruifeng920, ouyangsheng, huayitang, liuyonggsai}@ruc.edu.cn

ABSTRACT

Attention-based Transformers have demonstrated strong adaptability across a wide range of tasks and have become the backbone of modern Large Language Models (LLMs). However, their underlying mechanisms remain open for further exploration. The energy-based perspective has long provided a valuable principle for understanding neural computation. In this paper, we revisit the principle of energy as a lens to understand attention-based Transformer models. We present a unified energy-based framework which is composed of three key components: the local energy E_i , the global energy F , and the employed optimization algorithms. We show that different attention forms including unnormalized linear attention, gated linear attention and standard softmax attention can be induced by choosing their corresponding recipes within this framework. Building on this framework, we propose energy-based modifications of attention structures. Inspired by classical gradient descent (GD) algorithms, we extend the original attention formulation based on standard GD to the momentum-based GD, Nesterov Accelerated Gradient (NAG), and Newton’s method, each inducing a corresponding new attention structure. Our experiments provide preliminary support for the potential of the energy-based framework for designing attention mechanisms.

1 INTRODUCTION

In recent years, pretrained large language models (LLMs) have achieved remarkable success across various areas (Kenton & Toutanova, 2019; Brown et al., 2020). This success is not only attributed to these effective training paradigms such as auto-regressive pretraining but also relies on the attention-based Transformer architecture as the foundational backbone (Vaswani et al., 2017). Therefore, many studies have begun to explore the theoretical interpretations underlying the attention-based structures, with a popular approach being to connect the model architecture to unrolled optimization (Gregor & LeCun, 2010; Tolooshams & Ba, 2021; Chan et al., 2022; Hinton, 2022; Guo et al., 2023). The core idea of the unrolled optimization is to interpret the layer-wise forward computation of a model as performing an iterative optimization on some implicit objective function, which often corresponds to a mechanistic explanation. Yang et al. (2022) viewed Transformers composed of self-attention layers and the feed-forward network (FFN) layers as the unfolding of an interpretable optimization process across iterations by defining an energy function. Zhou et al. (2022) explained that stacked self-attention modules can promote grouping and noise filtering using the information bottleneck principle. Hoover et al. (2023) proposed the Energy Transformer, which uses attention-based layers designed to minimize a carefully constructed energy function. Yu et al. (2024b) showed that Transformer-like deep network layers can naturally be connected to an optimization process aimed at sparse rate reduction. Wang et al. (2025b) pointed out that compressing noisy token representations and the corresponding denoising operations can naturally give rise to the form of multi-head self-attention. Hu et al. (2025) presented an alternative to Transformers by quantifying semantic alignment and distributional uniformity with extended Hopfield energy functions. Actor et al. (2025) showed that optimizing latent features in multinomial regression align with dynamics induced by the attention blocks. These works provide comparable explanations for

*Corresponding author

attention-based architectures from different perspectives and often focus on specific attention forms with certain priors.

On the other hand, energy-based formulations have long underpinned theories of neural computation and the modeling of neural networks (Hopfield, 1982; Ackley et al., 1985; LeCun et al., 2006). One of the most influential works applying the concept of energy to pattern recognition is Associative Memory models, also known as Hopfield Networks Hopfield (1982; 1984), which implement associative memory by defining an energy function over neuron states. Modern Hopfield Networks have been largely enhanced to achieve greater storage capacity through the design of new energy functions (Krotov & Hopfield, 2016; Ramsauer et al., 2020; Krotov & Hopfield, 2020; Krotov, 2023). Additionally, based on the energy concept, LeCun et al. (2006) propose Energy-Based Models (EBMs) as a unifying framework for learning, where the training objective is to assign low energy to plausible configurations of variables and high energy to implausible ones. In fact, many modern self-supervised learning (SSL) methods can be naturally interpreted within this framework (Chen et al., 2020; He et al., 2020; LeCun, 2022; Gladstone et al., 2025). The energy-based perspective has demonstrated great appeal in the development of deep neural networks.

Previous works related to modern Hopfield networks also connects the concept of energy with forms of attention (Ramsauer et al., 2020; Krotov & Hopfield, 2020; Hu et al., 2023; 2024; Wu et al., 2023; 2024; Santos et al., 2024; Hoover et al., 2023). For instance, Ramsauer et al. (2020) proposed a modern Hopfield network whose energy function corresponds to an update rule that takes a form similar to the attention mechanism in Transformers. Hu et al. (2023); Wu et al. (2023) further proposed the energy functional regularized by entropy for sparse modern Hopfield models and show their dynamics takes the form of a broad family of attention rules including sparse attentions (Peters et al., 2019; Correia et al., 2019). In addition, Hu et al. (2024) connects the nonparametric modern Hopfield models to the efficient or approximate attention variants. These works either focus mainly on the associative memory capabilities of the modern Hopfield models or provide explanations of existing attention components, lacking a unified and generalizable framework for new attention architecture designs.

In this paper, we revisit the concept of energy to view attention-based Transformer models. Our work mainly follows the following line of presentation:

(a) Energy-based Framework for Attentions. We present an energy-based framework to provide a principled understanding of attention-based models in Section 2. This framework has three key components: the local energy E_i , the global energy F , and the used optimization algorithm. The local energy models the interactions between tokens, the global energy defines how the local energy is combined, and the optimization algorithm indicates how we optimize this global energy. We can choose different recipes within this framework to get different forms of attention, including unnormalized linear attention, gated linear attention, and standard softmax attention. Moreover, this framework not only provides options for understanding existing attention forms but also offers possibilities for designing potential attention forms: by selecting different ingredients, we can combine them to create new attention forms.

(b.) Energy-based Attention Modifications. Furthermore, we propose that the attention structure can be modified based on this energy-based framework in Section 3. We draw inspiration from existing GD algorithms to improve the attention structures. Specifically, in Section 3.1, we extend the vanilla GD form to momentum-based GD and Nesterov Accelerated Gradient (NAG), which correspond to the newly induced attention structures MomenMHA and NagMHA, respectively. Furthermore, in Section 3.2, we extend the 1st-order GD to a 2nd-order form grounded in Newton's method and then employ a Taylor expansion approximation to reduce its computational cost to the same order as standard attention. The induced new attention structure MHA2nd1st and its light version LightMHA2nd1st use the covariance matrix to precondition the original update directions, allowing tokens to adaptively adjust their movements along different dimensions. Finally, in Section 4, we conduct experiments to provide preliminary support for the potential of improving attention structures within the energy-based framework.

Table 1: Comparison of different attention forms under the energy-based framework.

Global Energy F	Local Energy E_i	Algorithm	Induced Attention
$-\frac{T}{2} \sum_i E_i^2$	$ \mathbf{z}^T \mathbf{W} \mathbf{h}_i $	1st-order GD	Linear Attention
$-\frac{T}{2} \sum_i \gamma_i E_i^2$	$ \mathbf{z}^T \mathbf{W} \mathbf{h}_i $	1st-order GD	Gated Linear Attention
$-T \log \sum_i e^{-E_i/T}$	$\frac{1}{2} \ \mathbf{z} - \mathbf{W} \mathbf{h}_i\ ^2$ or $-\mathbf{z}^T \mathbf{W} \mathbf{h}_i$	1st-order GD	Softmax Attention
		Momentum GD	MomenMHA
$-T \log \sum_i e^{-E_i/T}$	$\frac{1}{2} \ \mathbf{z} - \mathbf{W} \mathbf{h}_i\ ^2$ or $-\mathbf{z}^T \mathbf{W} \mathbf{h}_i$	Nesterov GD	NagMHA
		Newton's Method	MHA2nd

2 UNIFYING ATTENTION VIA ENERGY-BASED FRAMEWORK

For a given input $\mathbf{z} \in \mathbb{R}^d$, we assume that the set of tokens interacting with it is $\mathbf{H} = [\mathbf{h}_1, \dots, \mathbf{h}_N] \in \mathbb{R}^{d \times N}$. The core idea of the unrolled optimization is to treat the forward computation of the model as optimizing some implicit objective function, which can be formalized as:

$$\text{Forward process: } \hat{\mathbf{z}} = f_{\theta}(\mathbf{z}; \mathbf{H}) \iff \text{Implicit process: } \hat{\mathbf{z}} \approx \arg \min_{\mathbf{z}} F(\mathbf{z}; \mathbf{H}). \quad (1)$$

Here, the forward process involves a model $f_{\theta}(\mathbf{z}; \mathbf{H})$ parameterized by θ (e.g., attention-based models), which computes the update of the representation of \mathbf{z} given \mathbf{H} . This process can be equivalently viewed as implicitly optimizing an objective function $F(\mathbf{z}; \mathbf{H})$, whose specific form is typically determined by the model structure itself. For simplicity, we primarily consider the output $\hat{\mathbf{z}}$ corresponding to the input \mathbf{z} , assuming that the other tokens are static.

To illustrate how the form of attentions are related to the energy-based framework, we can first regard each token as a particle, with multiple particles together forming a system. We assume that there are already N particles within our system, and the position of the i -th particle in the system can be denoted by $\mathbf{h}_i \in \mathbb{R}^d$. We want to place a new particle $\mathbf{z} \in \mathbb{R}^d$ into the system and the other particles will exert interactions on it. The energy exerted by the i -th particle can be denoted as $E_i = E(\mathbf{z}, \mathbf{h}_i) \in \mathbb{R}$. We assume that the interaction of each particle on \mathbf{z} is independent, allowing us to express the global energy with respect to \mathbf{z} as $F : \mathbb{R}^N \rightarrow \mathbb{R}$ and its input is N -dimensional vector composed of E_i . Our goal is to find an appropriate \mathbf{z} that makes the global energy F as small as possible, i.e.,

$$\text{Implicit process: } \hat{\mathbf{z}} \approx \arg \min_{\mathbf{z}} F([E_1, \dots, E_N]) \quad \text{where } E_i = E(\mathbf{z}, \mathbf{h}_i). \quad (2)$$

Our observation is that when f_{θ} takes the form of attention models, the implicit optimization objective F in Eq (1) can be interpreted as the global energy function described above. The above Eq (2) roughly describes our energy-based framework; however, there are still many details to be specified. For instance, which form should the global energy F take to combine the local energy E_i ? How should the local energy E_i model the interactions between tokens? What algorithm should we use to perform this optimization process? We will illustrate on the design choices from three aspects:

- **Local Energy E_i** describes the form of interaction between particles (or tokens);
- **Global energy F** specifies how the individual energies E_i are combined;
- **Optimization Algorithm** outlines the update process of token representations.

These key components provide us with a recipe to understand different forms of attention: when different modifications are made to these components, corresponding attention architectures will be naturally induced. The framework is presented in Table 1. Next, we show how different attention forms (including unnormalized linear attention, standard softmax attention, etc.) can be derived from the above framework by making specific choices.

Case (i): Unnormalized Linear Attention

We begin with the simplest case of linear attention without normalization. Linear attentions are widely studied in the community due to its efficient computational performance (Tay et al., 2022). To achieve efficiency, linear attention replaces the exponential inner product form in the standard softmax attention with the standard inner product. The unnormalized linear attention with residual connection can be formalized as

$$\text{LA}(\mathbf{z}) = \mathbf{z} + \sum_{i=1}^N (\mathbf{z}^T \mathbf{W}_Q^T \mathbf{W}_K \mathbf{h}_i) \mathbf{W}_V \mathbf{h}_i, \quad (3)$$

where $\mathbf{W}_Q, \mathbf{W}_K, \mathbf{W}_V \in \mathbb{R}^{d \times d}$ are learnable parameters for query, key and value projection. In addition, although the original form of linear attentions such as Katharopoulos et al. (2020); Choromanski et al. (2020) included a normalization operation similar to softmax, subsequent works also show that this normalization method may lead to training instabilities (Qin et al., 2022; Dao & Gu, 2024). Therefore, here we also omit the normalization term here.

To see how unnormalized linear attention is related to the implicit optimization process in Eq (2), we give the following choices:

- Choice of local energy: Parametrized inner product absolute value form $E_i = |\mathbf{z}^T \mathbf{W} \mathbf{h}_i|$ where $\mathbf{W} \in \mathbb{R}^{d \times d}$ are the parameters to seek alignment in the semantic space.
- Choice of global energy: Negative sum of squares form $F = -\frac{T}{2} \sum_{i=1}^N E_i^2$ where T is the temperature.
- Choice of algorithm: One-step first-order gradient descent.

According to the above recipe, we can apply one-step gradient descent to minimize F

$$\begin{aligned} \hat{\mathbf{z}} &= \mathbf{z} - \eta \nabla_{\mathbf{z}} F = \mathbf{z} - \eta \nabla_{\mathbf{z}} \left(-\frac{T}{2} \sum_{i=1}^N E_i^2 \right) \\ &= \mathbf{z} + \sum_{i=1}^N ((\mathbf{z})^T \mathbf{W} \mathbf{h}_i) \eta T \mathbf{W} \mathbf{h}_i, \end{aligned}$$

where η is the learning rate. By comparing with Eq (3), we can set the learnable parameters in Eq (3) as $\mathbf{W}_Q^T \mathbf{W}_K = \mathbf{W}$ and further set $\mathbf{W}_V = \eta T \mathbf{W}$. Then, we will have $\text{LA}(\mathbf{z}) = \hat{\mathbf{z}}$.

Interestingly, under the above choices, the global energy without parameterization shares a very similar form with the classical Hopfield networks (Hopfield, 1982) whose energy function takes the form $E(\mathbf{z}) = -\frac{1}{2} \mathbf{z}^T \mathbf{H} \mathbf{H}^T \mathbf{z}$ with $\mathbf{z} \in \{\pm 1\}^d$ and the update rule $\mathbf{z}^{(t+1)} = \text{sign}(\mathbf{H} \mathbf{H}^T \mathbf{z}^{(t)})$. However, unlike its discrete update scenario, linear attention can be viewed as continuous updates of \mathbf{z} , with the residual connection (first-order gradient descent) playing the role of incremental updates. Moreover, it can be seen that the \mathbf{W} in local energy E_i is equivalent to $\mathbf{W}_Q^T \mathbf{W}_K$ in the attention layer, which are typically learned during training to find an appropriate semantic space. In addition, the learnable \mathbf{W}_V is often not limited to form $\mathbf{W}_V = \eta T \mathbf{W} = \eta T \mathbf{W}_Q^T \mathbf{W}_K$, making the model more flexible and powerful.

Case (ii): Gated Linear Attention

More recently, exploring more efficient architectural alternatives to the Transformer has become a key direction of research in the community (Yang et al., 2024; Wang et al., 2025a; Behrouz et al., 2024; 2025). Among these, gated variants of linear attention including RetNet (Sun et al., 2023), gated linear attention (Yang et al., 2023b), Gateloop (Katsch, 2023), xLSTM (Beck et al., 2024), LRU (Orvieto et al., 2023), HGRN (Qin et al., 2024), RWKV (Peng et al., 2023), etc., have attracted particular interest. More generally, these variants can be written as

$$\text{GLA}(\mathbf{z}) = \mathbf{z} + \sum_{i=1}^N \gamma_i (\mathbf{z}^T \mathbf{W}_Q^T \mathbf{W}_K \mathbf{h}_i) \mathbf{W}_V \mathbf{h}_i, \quad (4)$$

where γ_i is the factor that measures the importance of each token \mathbf{h}_i and may depend on the input \mathbf{z} at each step, in which case this can be seen as a forgetting gate. In addition, many recent works also

show that the state-specie models (SSMs) can also be regarded as members of gated linear attention family (Dao & Gu, 2024; Han et al., 2024; Ren et al., 2024). These forgetting factors are typically values between $[0, 1]$. In sequence modeling, different tokens are often assigned varying levels of importance based on the order of their occurrence in history. For instance, earlier tokens may have less influence on the present, leading their γ_i to approach 0.

In fact, in the case of linear attention, we only need to add the corresponding factor to the global energy to extend the recipe to the gated linear attention case. For completeness, we also provide the full choices here:

- Choice of local energy: Parametrized inner product absolute value form $E_i = |\mathbf{z}^T \mathbf{W} \mathbf{h}_i|$.
- Choice of global energy: Negative sum of squares form $F = -\frac{T}{2} \sum_{i=1}^N \gamma_i E_i^2$ where γ_i is the (data-dependent) scaling factor that measures the importance of each local energy.
- Choice of algorithm: One-step first-order gradient descent.

Case (iii): Standard Softmax Attention

The output of the standard softmax attention (SA) (Vaswani et al., 2017) in the single-head case can be formalized as

$$\text{SA}(\mathbf{z}) = \mathbf{z} + \mathbf{W}_V \mathbf{H} \text{softmax}(\mathbf{H}^T \mathbf{W}_K^T \mathbf{W}_Q \mathbf{z}) = \mathbf{z} + \sum_{i=1}^N \frac{e^{\mathbf{z}^T \mathbf{W}_Q^T \mathbf{W}_K \mathbf{h}_i / T}}{Z'} \mathbf{W}_V \mathbf{h}_i, \quad (5)$$

where T is the temperature and $\mathbf{W}_V, \mathbf{W}_K, \mathbf{W}_Q \in \mathbb{R}^{d \times d}$ are learnable parameters. In addition, $Z' = \sum_{j=1}^N e^{\mathbf{z}^T \mathbf{W}_Q^T \mathbf{W}_K \mathbf{h}_j / T}$ is the normalizing term. To see how the most widely used softmax attention is related to the implicit optimization process in Eq 1, we provide the following recipe:

- Choice of local energy: Parameterized ℓ_2 regression loss $E_i = \frac{1}{2} \|\mathbf{z} - \mathbf{W} \mathbf{h}_i\|^2$ when constrained by $\|\mathbf{z}\| = \|\mathbf{W} \mathbf{h}_i\| = \rho$, or equivalently, negative inner product $E_i = -\mathbf{z}^T \mathbf{W} \mathbf{h}_i$.
- Choice of global energy: the Helmholtz free energy form $F = -T \log \sum_{i=1}^N e^{-E_i / T}$.
- Choice of algorithm: One-step first-order gradient descent.

Based on the above choices, we apply one step of first-order gradient descent to F :

$$\begin{aligned} \hat{\mathbf{z}} &= \mathbf{z} - \eta \nabla_{\mathbf{z}} F = \mathbf{z} - \eta \nabla_{\mathbf{z}} \left(-T \log \sum_{i=1}^N e^{-\frac{\|\mathbf{z} - \mathbf{W} \mathbf{h}_i\|^2}{2T}} \right) \\ &= \mathbf{z} - \eta \nabla_{\mathbf{z}} \left(-T \log \sum_{i=1}^N e^{\frac{\mathbf{z}^T \mathbf{W} \mathbf{h}_i}{T}} + \rho^2 \right) \\ &= \mathbf{z} + \sum_{i=1}^N \frac{e^{\mathbf{z}^T \mathbf{W} \mathbf{h}_i / T}}{Z} \eta \mathbf{W} \mathbf{h}_i, \end{aligned}$$

where $Z = \sum_{j=1}^N e^{\mathbf{z}^T \mathbf{W} \mathbf{h}_j / T}$. By comparing with Eq (5), we can set the learnable parameters Eq (5) as $\mathbf{W}_Q^T \mathbf{W}_K = \mathbf{W}$ and $\mathbf{W}_V = \eta \mathbf{W}$. Then, we will have $Z' = Z$ and further $\text{SA}(\mathbf{z}) = \hat{\mathbf{z}}$.

It is worth noting that, under the above choices, the log-sum-exp form in the global energy is adopted by modern dense Hopfield networks (Ramsauer et al., 2020; Krotov & Hopfield, 2020). Hu et al. (2023); Wu et al. (2023) formalize the Helmholtz free-energy minimization principle for nonlinear attentions as an energy functional regularized by entropy and show that it induces a broad family of attention rules including softmax, sparsemax, and the more general α -entmax attentions (Martins & Astudillo, 2016; Peters et al., 2019; Correia et al., 2019). Later work connects efficient/approximate attention variants through a nonparametric framework (Hu et al., 2024).

As for the local energy, when we view it as an ℓ_2 regression loss, we impose a constraint on the norms of \mathbf{z} and $\mathbf{W} \mathbf{h}_i$, requiring them to lie on a hypersphere with radius ρ . This is similar to techniques used in practice, like QKNorm (Dehghani et al., 2023; Wortsman et al.), which stabilize the training of large Transformers. In fact, when this condition is relaxed to allow the vectors to

lie within the sphere $\|\mathbf{z}\| \leq \rho$, the above gradient descent process becomes an optimization of the upper bound of the global energy.

In addition, in the above incremental iterative update rule, the residual connection serves as the current iterate (solution), the parameterized component provides the search direction (update), and the final output can be viewed as the next iterate (solution). The parameters in attention can be viewed as learning to model the updating part (gradient) during training.

Discussion on More Ingredients:

In the above, we show how to make appropriate choices within the proposed framework and establish connections with existing major forms of attentions. In fact, modifications to the three key components in the existing scenario, namely local energy E_i , global energy F , and the optimization algorithm, can analogously lead to new forms of attention. Note that the three aspects mentioned above are relatively independent, meaning that different ingredients can be combined in various ways, leading to a rich variety of attention forms. Here, we discuss more existing or potential ingredients:

The local energy in the existing scenario is directly taken in the form of a parameterized inner product or ℓ_2 regression loss. Both can be viewed as a measure of similarity. A natural idea is to use a more general ℓ_p norm-based loss, that is, $E_i = \|\mathbf{z} - \mathbf{W}\mathbf{h}_i\|_p^p$ where $p \geq 1$ and $\|\cdot\|_p$ is the ℓ_p -norm for vectors. We may want to use different values of p depending on the data and scenario to achieve the desired properties. Additionally, another approach is that although the ℓ_2 -norm is a natural choice in many machine learning tasks, it is sensitive to outliers and extreme values. Therefore, it can be further extended to a more robust Huber loss-type (Huber, 1992; Hastie et al., 2009; Behrouz et al., 2025), that is,

$$E_i = E(\mathbf{z}, \mathbf{h}_i) = \begin{cases} \frac{1}{2}\|\mathbf{z} - \mathbf{W}\mathbf{h}_i\|^2 & \|\mathbf{z} - \mathbf{W}\mathbf{h}_i\| \leq \delta \\ \delta(\|\mathbf{z} - \mathbf{W}\mathbf{h}_i\| - \frac{1}{2}\delta) & \|\mathbf{z} - \mathbf{W}\mathbf{h}_i\| > \delta \end{cases}$$

where δ is a threshold. This loss function reduces the impact of outliers by applying a linear loss for large deviations. We leave it to further exploration whether these potential choices could enhance the attention structure in certain situations.

For global energy, existing literatures on sparse modern Hopfield networks (Hu et al., 2023; Wu et al., 2023) have established a generalized sparse Hopfield energy function, where Tsallis α -entropies (Tsallis, 1988) are used to yield retrieval dynamics corresponding to various sparse attentions. Softmax attention and sparsemax attention can be viewed as special cases with $\alpha = 1$ and $\alpha = 2$ respectively (Martins & Astudillo, 2016; Peters et al., 2019). More general values of α can lead to attention structures with varying degrees of sparsity (Correia et al., 2019). In addition, norm γ -negentropies can also be used to derive attention patterns different from the sparse attention modes above, where $\gamma = 1$ corresponds to agrmax, while $\gamma \rightarrow +\infty$ encourages sparse and uniform attention scores (Blondel et al., 2020; Santos et al., 2024).

As for the optimization algorithm, one-step first-order gradient descent is mainly used in the recipes of the discussed different attention forms. In fact, since there are lots of mature works in optimization literatures, it is possible for us to achieve this by drawing on these works. We will explore this in the next section to induce new forms of attention.

3 ENERGY-BASED MODIFICATIONS OF ATTENTION

In this section, we consider how existing attention mechanisms can be modified by changing the optimization algorithm in the energy-based framework proposed in Section 2. We primarily focus on modifications to the most commonly used softmax attention. Before that, we first present the definition of standard softmax attention in the multi-head setting:

$$\text{MHA}(\mathbf{z}) = \mathbf{z} + \sum_{h=1}^H \sum_{i=1}^N \frac{e^{\mathbf{z}^T \mathbf{W}_{Q,h}^T \mathbf{W}_{K,h} \mathbf{h}_i / T}}{Z'_h} \mathbf{W}_{O,h} \mathbf{W}_{V,h} \mathbf{h}_i, \quad (6)$$

where $\mathbf{W}_{V,h}, \mathbf{W}_{K,h}, \mathbf{W}_{Q,h} \in \mathbb{R}^{d_h \times d}$ and $\mathbf{W}_{O,h} \in \mathbb{R}^{d \times d_h}$ are learnable parameters. In addition, we have $d_h = \frac{d}{H}$ for each head and $Z'_h = \sum_{j=1}^N e^{\mathbf{z}^T \mathbf{W}_{Q,h}^T \mathbf{W}_{K,h} \mathbf{h}_j / T}$ as normalizing terms. Conceptually, multi-head attention works by first projecting tokens into lower-dimensional subspaces to

capture information independently and finally combining these representations back into the original d -dimensional space through the projection $\mathbf{W}_{O,h}$. Correspondingly, we use $E_{h,i}$ to denote the local energy between \mathbf{z} and \mathbf{h}_i in the h -th subspace. We provide the following recipe:

- Choice of local energy: Parameterized ℓ_2 regression loss $E_{h,i} = \frac{1}{2}\|\mathbf{W}_{1,h}\mathbf{z} - \mathbf{W}_{2,h}\mathbf{h}_i\|^2$ when constrained by $\|\mathbf{W}_{1,h}\mathbf{z}\| = \|\mathbf{W}_{2,h}\mathbf{h}_i\| = \rho$, or equivalently, negative inner product $E_i = -\mathbf{z}^T \mathbf{W}_{1,h}^T \mathbf{W}_{2,h} \mathbf{h}_i$, where $\mathbf{W}_{1,h}, \mathbf{W}_{2,h} \in \mathbb{R}^{d \times d_h}$ are parameters.
- Choice of global energy: the average Helmholtz free energy over the H subspaces $F = -\frac{1}{H} \sum_{h=1}^H T \log \sum_{i=1}^N e^{-E_{h,i}/T}$.
- Choice of algorithm: One-step first-order gradient descent.

According to the choices, we apply one step first-order gradient descent to F :

$$\begin{aligned} \hat{\mathbf{z}} &= \mathbf{z} - \eta \nabla_{\mathbf{z}} F = \mathbf{z} - \eta \nabla_{\mathbf{z}} \left(-\frac{1}{H} \sum_{h=1}^H T \log \sum_{i=1}^N e^{-\frac{\|\mathbf{W}_{1,h}\mathbf{z} - \mathbf{W}_{2,h}\mathbf{h}_i\|^2}{2T}} \right) \\ &= \mathbf{z} - \eta \nabla_{\mathbf{z}} \left(-\frac{1}{H} \sum_{h=1}^H T \log \sum_{i=1}^N e^{-\frac{\mathbf{z}^T \mathbf{W}_{1,h}^T \mathbf{W}_{2,h} \mathbf{h}_i}{T}} + \rho^2 \right) \\ &= \mathbf{z} + \sum_{h=1}^H \sum_{i=1}^N \frac{e^{\mathbf{z}^T \mathbf{W}_{1,h}^T \mathbf{W}_{2,h} \mathbf{h}_i / T}}{Z_h} \frac{\eta}{H} \mathbf{W}_{1,h}^T \mathbf{W}_{2,h} \mathbf{h}_i \end{aligned}$$

where $Z_h = \sum_{j=1}^N e^{\mathbf{z}^T \mathbf{W}_{1,h}^T \mathbf{W}_{2,h} \mathbf{h}_j / T}$. Comparing with Eq (6), we can set $\mathbf{W}_{1,h}^T \mathbf{W}_{2,h} = \mathbf{W}_{Q,h}^T \mathbf{W}_{K,h}$ and $\mathbf{W}_{O,h} \mathbf{W}_{V,h} = \frac{\eta}{H} \mathbf{W}_{1,h}^T \mathbf{W}_{2,h}$ for $h \in [H]$. Then, we will have $Z'_h = Z_h$ and $\text{MHA}(\mathbf{z}) = \hat{\mathbf{z}}$. The remaining discussion is similar to that of single-head softmax attention in Section 2.

In Section 2, we show that in our proposed energy-based framework, different combinations of the three key components will naturally give rise to corresponding attention forms, which serves as guidance for us in designing potential attention models. A natural idea then arises: if the forward pass of the attention mechanism can be viewed as optimizing the global energy F by one step first-order gradient descent (GD), can we directly obtain the final solution as the token representation (i.e., $\mathbf{z}^* = \text{argmin}_{\mathbf{z}} F$) instead of relying on such an incremental structure driven by local gradient descent? Unfortunately, except in certain special cases (e.g., \mathbf{h}_i are symmetrically distributed), it is difficult to directly obtain a closed-form analytical solution for F or its upper bound \tilde{F} . We present Lemma 1 as follows.

Lemma 1. *Both the global energy F and its upper bound \tilde{F} are non-convex with respect to \mathbf{z} . Assuming $\|\mathbf{W}_{1,h}\mathbf{z}\| \leq \rho$ and $\|\mathbf{W}_{2,h}\mathbf{h}_i\| \leq \rho$ for all $i \in [N]$ and $h \in [H]$, the local minima of F are attained at the boundary $\|\mathbf{W}_{1,h}\mathbf{z}\| = \rho$ or when $\sum_{h=1}^H \sum_{i=1}^N p_{i,h} \mathbf{W}_{1,h}^T (\mathbf{W}_{1,h}\mathbf{z} - \mathbf{W}_{2,h}\mathbf{h}_i) = 0$ where $p_{i,h} = \frac{1}{Z_h} e^{-\|\mathbf{W}_{1,h}\mathbf{z} - \mathbf{W}_{2,h}\mathbf{h}_i\|^2 / 2T}$ and $Z_h = \sum_{i=1}^N e^{-\|\mathbf{W}_{1,h}\mathbf{z} - \mathbf{W}_{2,h}\mathbf{h}_i\|^2 / 2T}$. In addition, the local minima of \tilde{F} are attained when $\|\mathbf{W}_{1,h}\mathbf{z}\| = \rho$.*

The proof of Lemma 1 is in Appendix A.2. The core is to show the Hessian matrix of F as

$$\nabla_{\mathbf{z}}^2 F = \frac{1}{H} \sum_{h=1}^H \underbrace{\left[\mathbf{W}_{1,h}^T \mathbf{W}_{1,h} - \frac{1}{T} \left(\sum_{i=1}^N p_{i,h} \mathbf{r}_{i,h} \mathbf{r}_{i,h}^T - (\nabla_{\mathbf{z}} F_h^*) (\nabla_{\mathbf{z}} F_h^*)^T \right) \right]}_{\succeq 0} \underbrace{\succeq 0}_{\preceq 0}, \quad (7)$$

which is composed of a positive semidefinite identity matrix and a negative semidefinite term for each head. Therefore, F is neither convex nor concave and its local minima can only occur at the boundary or at stationary points. Similarly, the Hessian of \tilde{F} contains only the negative semidefinite term, making it concave and ensuring that its local minima occur only on the boundary.

Although a closed-form solution is difficult to obtain directly in both cases, it is possible to obtain a better solution as the token representation by adopting more efficient GD algorithms within the energy-based framework, which in turn leads to improvements in the attention structure. In the following, we design modifications to the attention mechanism based on first-order and second-order gradient descent algorithms respectively.

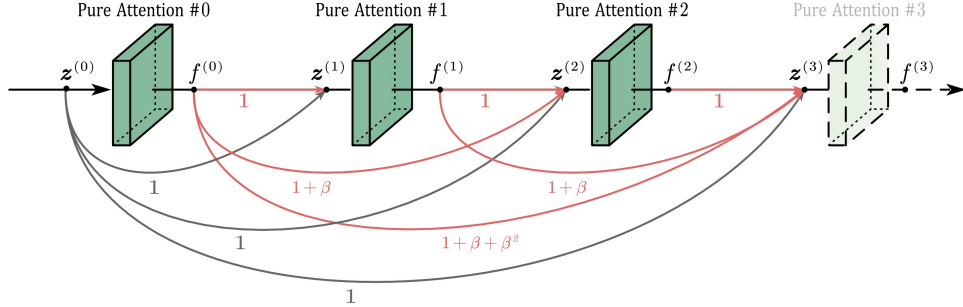


Figure 1: The illustration of the skip connections induced by MomenMHA. We show the computation of $z^{(L)}$ in the case $L = 3$ and $\eta = 1$. The output $z^{(k)}$ of the k -th layer can be viewed as a weighted sum of the initial input $z^{(0)}$ (shown in gray) and the pure attention outputs $f^{(k)}$ from the previous $k - 1$ layers (shown in pink). The weight of each skip connection is indicated next to it.

3.1 MODIFICATIONS BASED ON 1ST-ORDER GD

The original softmax attention in Eq (6) can be viewed as performing one step first-order GD, i.e.,

$$z^{(k+1)} = \text{MHA}(z^{(k)}) = z^{(k)} - \eta \nabla_{z^{(k)}} F,$$

where the update part can be viewed as modeling the gradient part $-\nabla_{z^{(k)}} F$ with $\eta = 1$. Considering the extensive literatures on GD, we can readily draw inspiration from them to inform modifications. The momentum-based GD algorithm (Sutskever et al., 2013) can be written as¹

$$\begin{cases} p^{(k+1)} = \beta p^{(k)} + \nabla_{z^{(k)}} F, \\ z^{(k+1)} = z^{(k)} - \eta p^{(k+1)}, \end{cases} \quad (8)$$

where p denotes the momentum and is initialized as $p^{(0)} = \mathbf{0}$, β is the momentum coefficient controlling the decay of past gradients, and η is the learning rate. By comparing the momentum-based GD with the original softmax attention update derived from vanilla GD, we can find that it suffices to replace $\nabla_{z^{(k)}} F$ in Eq (8) with the update part in Eq (6), that is,

$$\nabla_{z^{(k)}} F = - \sum_{h=1}^H \sum_{i=1}^N \frac{e^{(z^{(k)})^T \mathbf{W}_{Q,h}^T \mathbf{W}_{K,h} \mathbf{h}_i / T}}{Z'_h} \mathbf{W}_{O,h} \mathbf{W}_{V,h} \mathbf{h}_i = -f^{(k)},$$

where $T = \sqrt{d_h}$ and we use $f^{(k)}$ to denote the pure attention part (without skip connection). We set β and η as learnable parameters initialized to 0.9 and 1.0 respectively. We refer to this momentum-based modified structure as MomenMHA. Intuitively, the original attention mechanism can be viewed as modeling the gradient updates directly, whereas MomenMHA can be seen as learning the momentum updates. In fact, we can expand the update of z in Eq (8) to obtain

$$z^{(L)} = z^{(0)} + \sum_{k=0}^{L-1} \sum_{n=0}^{L-1-k} \eta \beta^n (-\nabla_{z^{(k)}} F) = z^{(0)} + \sum_{k=0}^{L-1} \left(\sum_{n=0}^{L-1-k} \eta \beta^n \right) f^{(k)}.$$

We can see that the output of the L -th layer can be viewed as a weighted sum of the initial input $z^{(0)}$ and the pure attention outputs $f^{(k)}$ from the previous $L - 1$ layers. This is equivalent to implicitly introducing L skip connections, which finally results in $\frac{L(L+1)}{2}$ skip connections across the L layers, which can be seen in Figure 1. This idea is closely related to that of DenseNet (Huang et al., 2017); however, in our case, these skip connections are introduced **implicitly** through the maintenance of a momentum vector p , and each skip connection is assigned a weight that follows **geometric series in β^n** with the inter-layer distance. In addition, in DenseNet, additional feature maps from different

¹It should be noted that here we put the learning rate η in the update of z , which is slightly different from Sutskever et al. (2013), where η appears in front of the gradient. A similar modification is also applied in the Nesterov Accelerated GD formulation. This form is closer to a PyTorch-style optimizer (torch.optim.SGD) implementation.

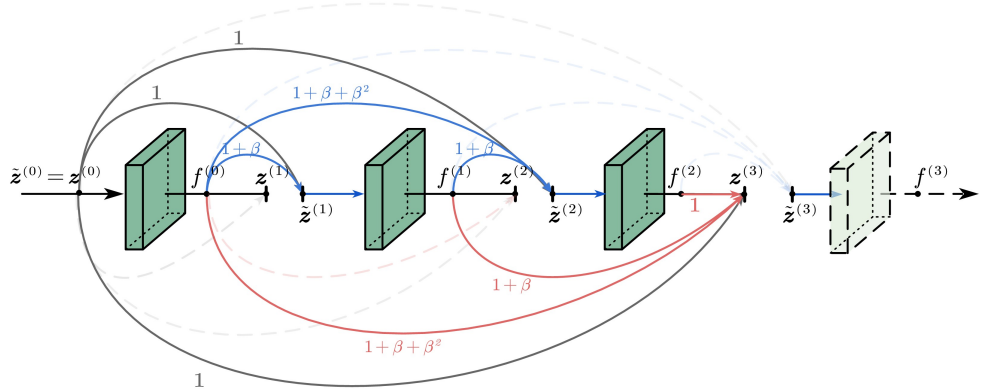


Figure 2: The illustration of the skip connections induced by NagMHA. We show the computation of $z^{(L)}$ in the case $L = 3$ and $\eta = 1$. Solid lines denote the skip connections that actually contribute to $z^{(3)}$, and the arrow directions indicate the flow of information. By introducing lookahead output $\tilde{z}^{(k)}$, additional nodes are incorporated into the information flow, resulting in denser extra skip connections compared to MomenMHA.

layers are concatenated and fed into the next layer, whereas in our approach the different features are directly added together.

Compared with the original attention form, MomenMHA needs to maintain a momentum vector p with the same shape as the input during the forward computation, thus introducing little additional overhead. In fact, prior work (Sander et al., 2021) has shown that maintaining an additional momentum vector can help reduce memory storage during backpropagation, since activations can be reconstructed on the fly during the backward pass, thereby offering potential savings in storage. We leave a detailed exploration of this implementation to future work. In addition, to enable the momentum p to propagate through the Feed-Forward Network layer as well, we apply a similar treatment to the FFN layer, that is, replacing $\nabla_{z^{(k)}} F$ with the output of the FFN module similarly.

Another GD variant to further accelerate the convergence is using Nesterov Accelerated Gradient (NAG) (Sutskever et al., 2013), which introduces a lookahead mechanism that estimates the future position before computing the gradient. This can be formalized as

$$\begin{cases} \tilde{z}^{(k)} = z^{(k)} - \beta p^{(k)}, \\ p^{(k+1)} = \beta p^{(k)} + \nabla_{\tilde{z}^{(k)}} F, \\ z^{(k+1)} = z^{(k)} - \eta p^{(k+1)}, \end{cases} \quad (9)$$

where $\tilde{z}^{(k)}$ denotes the lookahead (or predicted) position obtained by moving along the momentum direction. Similar to MomenMHA, we just need to replace $\nabla_{\tilde{z}^{(k)}} F$ with the update component from MHA and we call this modification as NagMHA. We use $\tilde{f}^{(k)}$ to denote the pure attention part with the input $\tilde{z}^{(k)}$. In fact, we can also expand \tilde{z} and z to obtain

$$\begin{cases} \tilde{z}^{(L)} = z^{(0)} - \sum_{k=0}^{L-1} \left(\eta \sum_{n=0}^{L-1-k} \beta^n + \beta^{L-k} \right) \nabla_{\tilde{z}^{(k)}} F = z^{(0)} + \sum_{k=0}^{L-1} \left(\eta \sum_{n=0}^{L-1-k} \beta^n + \beta^{L-k} \right) \tilde{f}^{(k)}, \\ z^{(L)} = z^{(0)} + \sum_{k=0}^{L-1} \sum_{n=0}^{L-1-k} \eta \beta^n (-\nabla_{\tilde{z}^{(k)}} F) = z^{(0)} + \sum_{k=0}^{L-1} \left(\sum_{n=0}^{L-1-k} \eta \beta^n \right) \tilde{f}^{(k)}. \end{cases}$$

The illustration of the skip connections induced by NagMHA is shown in Figure 2. When we focus only on the final output $z^{(L)}$, NagMHA can be viewed as introducing $L + (L+2)(L-1)/2$ useful skip connections, which is $L-1$ more than the $L(L+1)/2$ skip connections in MomenMHA. This is achieved by incorporating lookahead representations $\tilde{z}^{(k)}$. A more complete relationships among the skip connections is illustrated in Figure 3. In practice, the remaining design details and discussions are similar to those in MomenMHA, and are thus omitted for brevity.

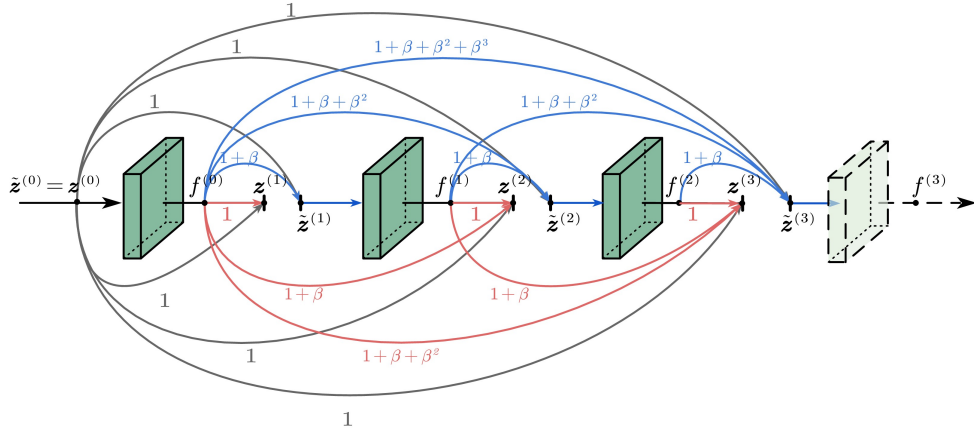


Figure 3: The illustration of the skip connections induced by NagMHA when $L = 3$ and $\eta = 1$. The lookahead output $\tilde{z}^{(k)}$ forms upper-side skip connections (shown in blue), which are used as inputs at each layer to estimate the gradients, while the skip connections used for computing $z^{(k)}$ are formed from the lower side (shown in pink). The gray lines are used to indicate the connections to the initial input $z^{(0)}$. The weight of each skip connection is indicated next to it. By introducing $\tilde{z}^{(k)}$, additional nodes are incorporated into the information flow, resulting in denser extra skip connections compared to MomenMHA.

3.2 MODIFICATIONS BASED ON NEWTON'S METHOD

In addition to first-order momentum-based methods, another simple and straightforward idea for employing a more efficient algorithm is to use Newton's method, which leverages the second-order information from the Hessian matrix to accelerate convergence. This can be formulated as

$$z^{(k+1)} = z^{(k)} - \eta [\nabla_{z^{(k)}}^2 F]^{-1} \nabla_{z^{(k)}} F,$$

where $\nabla_{z^{(k)}}^2 F$ is the Hessian matrix at $z^{(k)}$. The above update can be viewed as preconditioning the gradient with the Hessian matrix to accelerate convergence. We denote the Helmholtz free energy in the h -th subspace as $F_h = -T \log \sum_{i=1}^N Z_h$ and then $F = \frac{1}{H} F_h$. Instead of applying Newton's method directly to F , we apply it independently to each subspace F_h , which can be formalized as

$$z^{(k+1)} = z^{(k)} - \frac{\eta}{H} \sum_{h=1}^H [\nabla_{z^{(k)}}^2 F_h]^{-1} \nabla_{z^{(k)}} F_h.$$

Considering the analogous roles of $\mathbf{W}_{1,h}^T \mathbf{W}_{2,h}$ and $\mathbf{W}_{Q,h}^T \mathbf{W}_{K,h}$ in the recipe of multi-head softmax attention, we use the notation $\mathbf{q}_h = \mathbf{W}_{1,h} z$, $\mathbf{k}_{i,h} = \mathbf{W}_{2,h} \mathbf{h}_i$ and $\bar{\mathbf{k}}_h = \sum_{i=1}^N p_{i,h} \mathbf{W}_{2,h} \mathbf{h}_i$ where $p_{i,h} = \frac{1}{Z_h} e^{-\|\mathbf{W}_{1,h} z - \mathbf{W}_{2,h} \mathbf{h}_i\|^2 / 2T}$. Then the Hessian matrix of F_h is

$$\nabla_{\mathbf{z}}^2 F_h = \mathbf{W}_{1,h}^T \left[\mathbf{I} - \frac{1}{T} \sum_{i=1}^N p_{i,h} (\mathbf{k}_{i,h} - \bar{\mathbf{k}}_h) (\mathbf{k}_{i,h} - \bar{\mathbf{k}}_h)^T \right] \mathbf{W}_{1,h}.$$

Note that due to $\mathbf{W}_{1,h} \in \mathbb{R}^{d_h \times d}$, the Hessian matrix $\nabla_{\mathbf{z}}^2 F_h \in \mathbb{R}^{d \times d}$ is non-invertible. Therefore, we need to employ the range-space approach² to compute the inverse, which is equivalent to using the Moore–Penrose pseudoinverse. However, the inverse of the intermediate matrix incurs a cost of $O(d_h^3)$, which is often impractical in practice³. To further reduce the cost, we approximate the inverse using its Taylor expansion, that is,

$$\left[\mathbf{I} - \frac{1}{T} \sum_{i=1}^N p_{i,h} \mathbf{d}_{i,h} \mathbf{d}_{i,h}^T \right]^{-1} \approx \mathbf{I} + \frac{1}{T} \sum_{i=1}^N p_{i,h} \mathbf{d}_{i,h} \mathbf{d}_{i,h}^T + \frac{1}{T^2} \left(\sum_{i=1}^N p_{i,h} \mathbf{d}_{i,h} \mathbf{d}_{i,h}^T \right)^2 + \dots$$

²Here we use $(\mathbf{W}^T \mathbf{C} \mathbf{W})^\dagger = \mathbf{W}^T (\mathbf{W} \mathbf{W}^T)^{-1} \mathbf{C}^{-1} (\mathbf{W} \mathbf{W}^T)^{-1} \mathbf{W}$ when $\mathbf{W} \in \mathbb{R}^{m \times n}$ and $m < n$.

³Noting that the Hessian can be expressed as a sum of rank-1 perturbations, we can use the Sherman–Morrison–Woodbury formula to compute the inverse and the resulting cost is $O(N d_h^2)$. This will provide savings when $N \ll d_h$, but overall, the cost is still higher than the standard softmax attention.

where $d_{i,h} = k_{i,h} - \bar{k}_h$. Here, we retain only the first-order term. Finally, by parameterize $\mathbf{W}_{1,h}, \mathbf{W}_{2,h}$ as $\mathbf{W}_{Q,h}, \mathbf{W}_{K,h}$, the final modification can be formalized as

$$\begin{aligned} \text{MHA2nd1st}(\mathbf{z}) &= \mathbf{z} + \sum_{h=1}^H \mathbf{W}_{O,h} \mathbf{W}_{V,h} \mathbf{M}_h (\mathbf{q}_h - \bar{\mathbf{k}}_h + \mathbf{b}_h), \\ \mathbf{M}_h &= \mathbf{W}_{Q,h}^T (\mathbf{W}_{Q,h} \mathbf{W}_{Q,h}^T)^{-1}, \quad \mathbf{b}_h = \frac{1}{T} \sum_{i=1}^N p_{i,h} \mathbf{d}_{i,h} [\mathbf{d}_{i,h}^T (\mathbf{q}_h - \bar{\mathbf{k}}_h)], \end{aligned}$$

where $\mathbf{W}_{O,h} \in \mathbb{R}^{d \times \frac{d}{H}}$, $\mathbf{W}_{V,h} \in \mathbb{R}^{\frac{d}{H} \times d}$ are parameters introduced to align with original MHA and the term $\frac{\eta}{H}$ is absorbed into these learnable parameters. We can see that the vector \mathbf{b}_h acts as a bias term, adjusting the update using variance information in the subspace. Moreover, to maintain stability, we set the temperature T in the attention score $p_{i,h}$ as a head-wise learnable parameter with initialization as $\sqrt{2d_h}$ and the temperature in \mathbf{b}_h is treated in the similar way. We denote this structure as MHA2nd1st(\mathbf{z}) as it is inspired by Newton's method while approximating the inverse using first-order Taylor expansion.

Note that although the computation of \mathbf{M}_h still involves a matrix inverse, it is shared across all queries and therefore only needs to be computed once, which does not introduce significant overhead. We can prioritize the computation of vector–vector inner products in \mathbf{b}_h to avoid performing matrix–vector multiplications. The total cost for H heads is $O(Nd + d^2)$, sharing the same asymptotic complexity as standard attention despite a larger constant factor.

In addition, since MHA2nd1st appears somewhat bulky, we also design a more light variant that succinctly retains its core idea: using the information in the covariance matrix to adjust the update for each dimension. The form of this light variant is given by

$$\begin{aligned} \text{LightMHA2nd1st}(\mathbf{z}) &= \mathbf{z} + \sum_{h=1}^H \mathbf{W}_{O,h} (\bar{\mathbf{v}}_h + \tau_h \mathbf{b}_h), \\ \bar{\mathbf{v}}_h &= \sum_{i=1}^N p_{i,h} \mathbf{W}_{V,h} \mathbf{h}_i, \quad \mathbf{b}_h = \sum_i^N p_{i,h} \mathbf{v}_{i,h} \mathbf{v}_{i,h}^T \bar{\mathbf{v}}_h - \bar{\mathbf{v}}_h \bar{\mathbf{v}}_h^T \bar{\mathbf{v}}_h, \end{aligned}$$

where $p_{i,h} = \frac{1}{Z_h} e^{\frac{\mathbf{z}^T \mathbf{W}_{Q,h}^T \mathbf{W}_{K,h} \mathbf{h}_i}{T}}$ and τ_h are learnable parameters for each head with initialization as $\tau_h = 0.01$. Compared with the original MHA2nd1st, this light version computes the attention scores using direct inner products instead of Euclidean distances. At the same time, we also adopt the **parameterization-then-preconditioning** strategy to make the formulation deviate as little as possible from the original MHA. More details about the derivation can be seen in Appendix A.3.

4 EXPERIMENTS

To explore the potential of the proposed attention modifications, we conduct experiments using a GPT-like architecture (Brown et al., 2020). Specifically, we replace the original standard softmax attention with the MomenMHA and NagMHA introduced in Section 3.1, as well as the MHA2nd1st and LightMHA2nd1st described in Section 3.2. The model sizes range from 30M to 160M parameters. Considering our limited computational resources (two 24GB NVIDIA GeForce RTX 3090 GPUs), we conduct pre-training on the MiniPile dataset (Kaddour, 2023), which is a compact subset version of the original Pile dataset (Gao et al., 2020). We use the GPT-2 tokenizer from huggingface (Wolf et al., 2020) to process the corpus. We conduct training on the training set containing 1 million samples with the objective of next-token prediction, while simultaneously monitoring and reporting the loss on the validation set. More experiment details can be seen in Appendix A.4.

As an initial validation of the proposed model, we choose a relatively short sequence length by truncating each training example to 256 tokens. We present the results of models with different sizes in Figure 4, where the red line represents the baseline using the standard softmax MHA. First, both MomenMHA and NagMHA achieve faster training convergence than the standard MHA across all model sizes, with NagMHA being the fastest among all variants. This observation is particularly

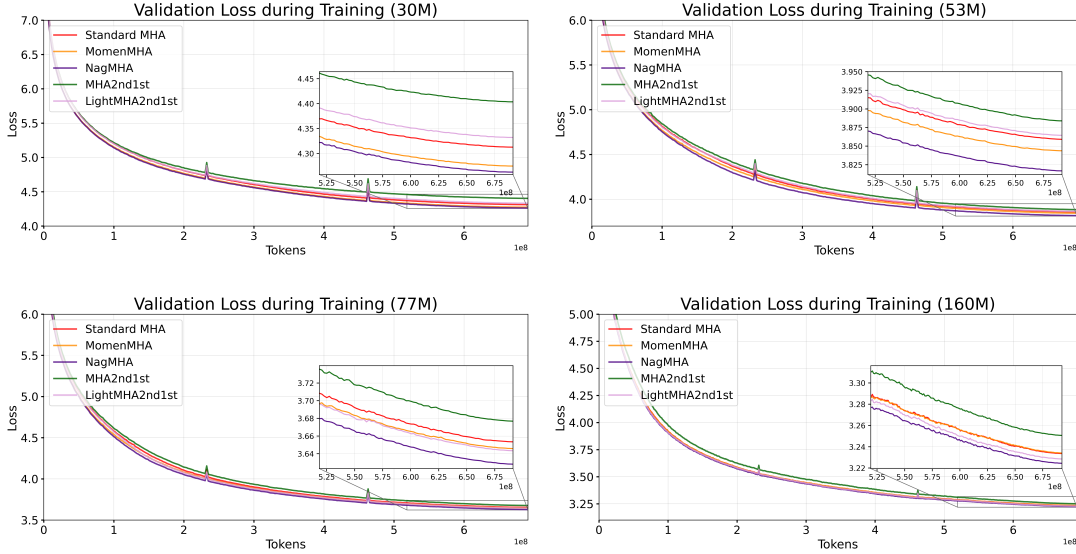


Figure 4: Validation loss on MiniPile during training for different modifications with a training window length of 256. MomenMHA and NagMHA show faster convergence than the standard MHA, with NagMHA being the most efficient. While MHA2nd1st underperforms due to its more complex formulation, the lightweight version LightMHA2nd1st achieves comparable or slightly better results at larger model scales.

interesting, as NAG is also theoretically proven to converge faster than vanilla SGD and momentum-based GD in optimization theory. We attribute this faster convergence to the more densely introduced skip connections. In contrast, MHA2nd1st consistently underperforms the standard MHA, which we attribute to the relatively complex bias vector b —the coupling among multiple inputs may increase the difficulty of optimization. Finally, the lightweight version LightMHA2nd1st performs comparably to the standard attention mechanism and even slightly faster for models with 77M and 160M parameters.

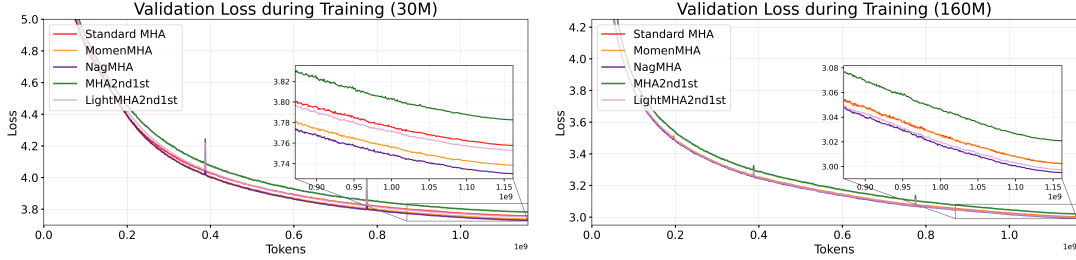


Figure 5: Validation loss on MiniPile during training for different modifications with a training window length of 512. MomenMHA and NagMHA show faster convergence than the standard MHA, with NagMHA being the most efficient. While MHA2nd1st underperforms due to its more complex formulation, the light version LightMHA2nd1st achieves comparable or slightly better results at larger model scales.

Furthermore, we extend the training sequence length from 256 to 512 and conduct pretraining under the same settings, with the results shown in Figure 5. As can be seen, when the model size is 30M, all attention variants except MHA2nd1st converge faster than the standard attention mechanism. When the model size is further scaled to 160M, MomenMHA becomes comparable to the original attention, while NagMHA and LightMHA2nd1st continue to exhibit faster convergence.

Furthermore, we perform instruction fine-tuning on various GLUE tasks (Wang et al., 2018) based on the 160M autoregressively trained models. We focus on classification tasks and exclude the

Table 2: Performance comparison across GLUE tasks. Mean accuracy is reported with standard deviation shown in smaller font.

Tasks	Standard MHA	MomenMHA	NagMHA	MHA2nd1st	LightMHA2nd1st
RTE	52.81 \pm 0.22	52.33 \pm 0.35	52.81 \pm 0.22	52.69 \pm 0.35	52.81 \pm 0.22
MRPC	69.85 \pm 0.49	71.49 \pm 0.37	70.67 \pm 0.62	71.65 \pm 0.14	70.75 \pm 0.71
CoLA	69.12 \pm 0.07	69.18 \pm 0.04	68.96 \pm 0.35	69.18 \pm 0.04	69.21 \pm 0.09
SST-2	87.16 \pm 0.35	87.39 \pm 1.22	87.31 \pm 0.75	87.28 \pm 0.91	87.73 \pm 0.12
QNLI	81.53 \pm 2.34	81.80 \pm 1.67	80.77 \pm 1.87	82.43 \pm 0.90	81.20 \pm 2.80
QQP	86.24 \pm 0.67	86.55 \pm 0.59	86.52 \pm 0.52	84.73 \pm 1.38	86.20 \pm 0.83
MNLI-M	73.06 \pm 1.49	73.79 \pm 0.98	73.75 \pm 1.13	72.47 \pm 0.35	72.87 \pm 1.60
MNLI-MM	73.67 \pm 1.15	74.16 \pm 0.85	74.15 \pm 0.89	73.61 \pm 0.25	73.50 \pm 1.23
Average	74.18	74.59	74.37	74.26	74.28

regression task STS-B as well as WNLI whose training set is too small. We conduct three runs with different random seeds and report the mean accuracy and standard deviation in Table 2. It can be observed that the momentum-based MomenMHA and NagMHA outperform the standard MHA with MomenMHA achieving the best overall performance. In addition, MHA2nd1st and its lightweight version also achieve slightly better performance than the standard MHA. Overall, these results provide preliminary support that the modified attention structure derived from the energy-based framework has the potential to achieve performance that is comparable to or exceeds that of the original softmax attention.

5 DISCUSSIONS ON RELATED WORK AND FUTURE DIRECTION

In this part, we discuss the related work and potential future directions in more detailed discussion.

Unrolled Optimization, Test-time Training and Design of Model Architecture: Understanding and designing model architectures from the perspective of unrolled optimization is a currently active area of research (Gregor & LeCun, 2010; Tolooshams & Ba, 2021; Chan et al., 2022; Guo et al., 2023). Previous works have designed and interpreted Transformer-like structures from various viewpoints, including sparse rate distortion (Yu et al., 2024b;a), denoising (Wang et al., 2025b), information bottleneck (Zhou et al., 2022), multinomial regression (Actor et al., 2025), etc. Yang et al. (2022); Hoover et al. (2023); Hu et al. (2025) also used the concept of energy to explain attention-based models. However, their attention is set in a self-attention structure, where all tokens evolve simultaneously, while we focus more on the cross-attention setting, where the other h_i are fixed during the update process of z . In addition, unlike previous works which focus more on interpreting specific attention-based architectures, our approach starts from the concept of energy to interpret different attention forms, and show that new attention structures can be designed based on the proposed energy framework.

We also note that designing efficient model architectures through test-time training (regression) framework, has recently become an active research area (Sun et al., 2024; von Oswald et al., 2025; Yang et al., 2024; Wang et al., 2025a; Behrouz et al., 2024). This framework focuses on the update of the memory module (function), typically represented by a matrix formed from a key-value outer product, while the update rules induced by our framework are applied to the token z as the object. We believe that, in the context of linear attentions, modifying the underlying energy functions, GD forms, or their combinations may correspond to some existing architectures and could inspire the design of new ones. Moreover, considering the extensive literature in optimization theory, we believe it offers a rich source of inspiration for developing new GD-form-guided designs.

Energy principle and Transformers: The concept of energy has long been used in deep neural networks (Hopfield, 1982; 1984; Ackley et al., 1985; Krotov & Hopfield, 2016; LeCun et al., 2006;

LeCun, 2022). The studies most relevant to ours are likely those related to modern Hopfield networks Ramsauer et al. (2020); Krotov & Hopfield (2020); Hu et al. (2023); Wu et al. (2023); Hu et al. (2024); Wu et al. (2024); Santos et al. (2024). For instance, Ramsauer et al. (2020); Krotov & Hopfield (2020) analyze the energy function that takes the log-sum-exp form for continuous-state Hopfield network whose update rule share the same form as the attention mechanism in the Transformer. Hu et al. (2023); Wu et al. (2023) proposed the energy functional regularized by entropy for the sparse modern Hopfield models and show that their dynamics corresponds to a broad family of attention rules including softmax, sparsemax, and the more general α -entmax attentions (Martins & Astudillo, 2016; Peters et al., 2019; Correia et al., 2019). Later work connected efficient attention variants through a nonparametric framework (Hu et al., 2024). Although we also use the concept of energy, energy itself is merely an interpretation of the implicit objective function in unrolled optimization, rather than the energy in the Hopfield model. Therefore, unlike the aforementioned works, we do not delve into a theoretical analysis of the modern Hopfield model’s capabilities. Our energy-based framework focus more on providing a unified perspective on the design of existing attention forms (including unnormalized linear attention, gated linear attention and standard softmax attention) with residual connections, as well as offering insights for the design of new structures. Furthermore, we note that Gladstone et al. (2025) employ energy-based methods to train Transformers and their focus is more related to training paradigms, which is orthogonal to our work.

Test-time Scaling and Loop Transformers: Test-time scaling is a favored pathway to boost model inference (Zhang et al., 2025; Snell et al., 2024; Muennighoff et al., 2025). Among these methods, Loop Transformers output token representations through parameter-shared recurrent computations and existing research demonstrates that this recurrent structure offers advantages in terms of performance gains and capability generalization (Geiping et al., 2025; Fan et al., 2024; Yang et al., 2023a; Yu et al., 2025; Altabaa et al., 2025; Wu et al., 2025; Zhu et al., 2025). These models can be viewed as neural networks that learn to perform fixed-point iterations, a concept explored in deep equilibrium models (Bai et al., 2019; 2021). Unlike stacking attention layers with distinct parameters, using parameter-shared recurrent computation aligns more closely with optimizing the same energy function within a relatively stable semantic space. We believe a potential direction is to connect fixed-point learning with the specific energy-based objective functions F . As for this, we put more discussions in Appendix A.1. In addition, exploring how advanced GD-inspired attention mechanisms (e.g., momentum-based GD, NAG, or Newton’s method) can be incorporated into Loop Transformers may further enhance the efficiency and stability of representation learning.

REFERENCES

David H Ackley, Geoffrey E Hinton, and Terrence J Sejnowski. A learning algorithm for boltzmann machines. *Cognitive science*, 9(1):147–169, 1985.

Jonas A Actor, Anthony Gruber, and Eric C Cyr. Interpreting transformer architectures as implicit multinomial regression. *arXiv preprint arXiv:2509.04653*, 2025.

Awni Altabaa, Siyu Chen, John Lafferty, and Zhuoran Yang. Unlocking out-of-distribution generalization in transformers via recursive latent space reasoning. *arXiv preprint arXiv:2510.14095*, 2025.

Shaojie Bai, J Zico Kolter, and Vladlen Koltun. Deep equilibrium models. *Advances in neural information processing systems*, 32, 2019.

Shaojie Bai, Vladlen Koltun, and J Zico Kolter. Neural deep equilibrium solvers. In *International Conference on Learning Representations*, 2021.

Maximilian Beck, Korbinian Pöppel, Markus Spanring, Andreas Auer, Oleksandra Prudnikova, Michael Kopp, Günter Klambauer, Johannes Brandstetter, and Sepp Hochreiter. xlstm: Extended long short-term memory. *Advances in Neural Information Processing Systems*, 37:107547–107603, 2024.

Ali Behrouz, Peilin Zhong, and Vahab Mirrokni. Titans: Learning to memorize at test time. *arXiv preprint arXiv:2501.00663*, 2024.

Ali Behrouz, Meisam Razaviyayn, Peilin Zhong, and Vahab Mirrokni. It's all connected: A journey through test-time memorization, attentional bias, retention, and online optimization. *arXiv preprint arXiv:2504.13173*, 2025.

Mathieu Blondel, André FT Martins, and Vlad Niculae. Learning with fenchel-young losses. *Journal of Machine Learning Research*, 21(35):1–69, 2020.

Tom Brown, Benjamin Mann, Nick Ryder, Melanie Subbiah, Jared D Kaplan, Prafulla Dhariwal, Arvind Neelakantan, Pranav Shyam, Girish Sastry, Amanda Askell, et al. Language models are few-shot learners. *Advances in neural information processing systems*, 33:1877–1901, 2020.

Kwan Ho Ryan Chan, Yaodong Yu, Chong You, Haozhi Qi, John Wright, and Yi Ma. Redunet: A white-box deep network from the principle of maximizing rate reduction. *Journal of machine learning research*, 23(114):1–103, 2022.

Ting Chen, Simon Kornblith, Mohammad Norouzi, and Geoffrey Hinton. A simple framework for contrastive learning of visual representations. In *International conference on machine learning*, pp. 1597–1607. PMLR, 2020.

Krzysztof Choromanski, Valerii Likhoshesterov, David Dohan, Xingyou Song, Andreea Gane, Tamas Sarlos, Peter Hawkins, Jared Davis, Afroz Mohiuddin, Lukasz Kaiser, et al. Rethinking attention with performers. *arXiv preprint arXiv:2009.14794*, 2020.

Gonçalo M Correia, Vlad Niculae, and André FT Martins. Adaptively sparse transformers. *arXiv preprint arXiv:1909.00015*, 2019.

Tri Dao and Albert Gu. Transformers are ssms: Generalized models and efficient algorithms through structured state space duality. *arXiv preprint arXiv:2405.21060*, 2024.

Mostafa Dehghani, Josip Djolonga, Basil Mustafa, Piotr Padlewski, Jonathan Heek, Justin Gilmer, Andreas Peter Steiner, Mathilde Caron, Robert Geirhos, Ibrahim Alabdulmohsin, et al. Scaling vision transformers to 22 billion parameters. In *International conference on machine learning*, pp. 7480–7512. PMLR, 2023.

Ying Fan, Yilun Du, Kannan Ramchandran, and Kangwook Lee. Looped transformers for length generalization. *arXiv preprint arXiv:2409.15647*, 2024.

Leo Gao, Stella Biderman, Sid Black, Laurence Golding, Travis Hoppe, Charles Foster, Jason Phang, Horace He, Anish Thite, Noa Nabeshima, et al. The pile: An 800gb dataset of diverse text for language modeling. *arXiv preprint arXiv:2101.00027*, 2020.

Jonas Geiping, Sean McLeish, Neel Jain, John Kirchenbauer, Siddharth Singh, Brian R Bartoldson, Bhavya Kailkhura, Abhinav Bhatale, and Tom Goldstein. Scaling up test-time compute with latent reasoning: A recurrent depth approach. *arXiv preprint arXiv:2502.05171*, 2025.

Alexi Gladstone, Ganesh Nanduru, Md Mofijul Islam, Peixuan Han, Hyeyoung Ha, Aman Chadha, Yilun Du, Heng Ji, Jundong Li, and Tariq Iqbal. Energy-based transformers are scalable learners and thinkers. *arXiv preprint arXiv:2507.02092*, 2025.

Karol Gregor and Yann LeCun. Learning fast approximations of sparse coding. In *Proceedings of the 27th international conference on international conference on machine learning*, pp. 399–406, 2010.

Xiaojun Guo, Yifei Wang, Tianqi Du, and Yisen Wang. Contranorm: A contrastive learning perspective on oversmoothing and beyond. *arXiv preprint arXiv:2303.06562*, 2023.

Dongchen Han, Ziyi Wang, Zhuofan Xia, Yizeng Han, Yifan Pu, Chunjiang Ge, Jun Song, Shiji Song, Bo Zheng, and Gao Huang. Demystify mamba in vision: A linear attention perspective. *arXiv preprint arXiv:2405.16605*, 2024.

Trevor Hastie, Robert Tibshirani, Jerome Friedman, et al. The elements of statistical learning, 2009.

Kaiming He, Haoqi Fan, Yuxin Wu, Saining Xie, and Ross Girshick. Momentum contrast for unsupervised visual representation learning. In *Proceedings of the IEEE/CVF conference on computer vision and pattern recognition*, pp. 9729–9738, 2020.

Dan Hendrycks and Kevin Gimpel. Gaussian error linear units (gelus). *arXiv preprint arXiv:1606.08415*, 2016.

Geoffrey Hinton. The forward-forward algorithm: Some preliminary investigations. *arXiv preprint arXiv:2212.13345*, 2(3):5, 2022.

Benjamin Hoover, Yuchen Liang, Bao Pham, Rameswar Panda, Hendrik Strobelt, Duen Horng Chau, Mohammed Zaki, and Dmitry Krotov. Energy transformer. *Advances in neural information processing systems*, 36:27532–27559, 2023.

John J Hopfield. Neural networks and physical systems with emergent collective computational abilities. *Proceedings of the national academy of sciences*, 79(8):2554–2558, 1982.

John J Hopfield. Neurons with graded response have collective computational properties like those of two-state neurons. *Proceedings of the national academy of sciences*, 81(10):3088–3092, 1984.

Jerry Yao-Chieh Hu, Donglin Yang, Dennis Wu, Chenwei Xu, Bo-Yu Chen, and Han Liu. On sparse modern hopfield model. *Advances in neural information processing systems*, 36:27594–27608, 2023.

Jerry Yao-Chieh Hu, Bo-Yu Chen, Dennis Wu, Feng Ruan, and Han Liu. Nonparametric modern hopfield models. *arXiv preprint arXiv:2404.03900*, 2024.

Yunzhe Hu, Difan Zou, and Dong Xu. Hyper-set: Designing transformers via hyperspherical energy minimization. *arXiv preprint arXiv:2502.11646*, 2025.

Gao Huang, Zhuang Liu, Laurens Van Der Maaten, and Kilian Q Weinberger. Densely connected convolutional networks. In *Proceedings of the IEEE conference on computer vision and pattern recognition*, pp. 4700–4708, 2017.

Peter J Huber. Robust estimation of a location parameter. In *Breakthroughs in statistics: Methodology and distribution*, pp. 492–518. Springer, 1992.

Jean Kaddour. The minipile challenge for data-efficient language models. *arXiv preprint arXiv:2304.08442*, 2023.

Angelos Katharopoulos, Apoorv Vyas, Nikolaos Pappas, and François Fleuret. Transformers are rnns: Fast autoregressive transformers with linear attention. In *International conference on machine learning*, pp. 5156–5165. PMLR, 2020.

Tobias Katsch. Gateloop: Fully data-controlled linear recurrence for sequence modeling. *arXiv preprint arXiv:2311.01927*, 2023.

Jacob Devlin Ming-Wei Chang Kenton and Lee Kristina Toutanova. Bert: Pre-training of deep bidirectional transformers for language understanding. In *Proceedings of naacl-HLT*, volume 1, pp. 2, 2019.

Dmitry Krotov. A new frontier for hopfield networks. *Nature Reviews Physics*, 5(7):366–367, 2023.

Dmitry Krotov and John Hopfield. Large associative memory problem in neurobiology and machine learning. *arXiv preprint arXiv:2008.06996*, 2020.

Dmitry Krotov and John J Hopfield. Dense associative memory for pattern recognition. *Advances in neural information processing systems*, 29, 2016.

Yann LeCun. A path towards autonomous machine intelligence version 0.9. 2, 2022-06-27. *Open Review*, 62(1):1–62, 2022.

Yann LeCun, Sumit Chopra, Raia Hadsell, M Ranzato, Fujie Huang, et al. A tutorial on energy-based learning. *Predicting structured data*, 1(0), 2006.

I Loshchilov. Decoupled weight decay regularization. *arXiv preprint arXiv:1711.05101*, 2017.

Andre Martins and Ramon Astudillo. From softmax to sparsemax: A sparse model of attention and multi-label classification. In *International conference on machine learning*, pp. 1614–1623. PMLR, 2016.

Niklas Muennighoff, Zitong Yang, Weijia Shi, Xiang Lisa Li, Li Fei-Fei, Hannaneh Hajishirzi, Luke Zettlemoyer, Percy Liang, Emmanuel Candès, and Tatsunori Hashimoto. s1: Simple test-time scaling. *arXiv preprint arXiv:2501.19393*, 2025.

Antonio Orvieto, Samuel L Smith, Albert Gu, Anushan Fernando, Caglar Gulcehre, Razvan Pascanu, and Soham De. Resurrecting recurrent neural networks for long sequences. In *International Conference on Machine Learning*, pp. 26670–26698. PMLR, 2023.

Bo Peng, Eric Alcaide, Quentin Anthony, Alon Albalak, Samuel Arcadinho, Stella Biderman, Huanqi Cao, Xin Cheng, Michael Chung, Matteo Grella, et al. Rwkv: Reinventing rnns for the transformer era. *arXiv preprint arXiv:2305.13048*, 2023.

Ben Peters, Vlad Niculae, and André FT Martins. Sparse sequence-to-sequence models. *arXiv preprint arXiv:1905.05702*, 2019.

Zhen Qin, Xiaodong Han, Weixuan Sun, Dongxu Li, Lingpeng Kong, Nick Barnes, and Yiran Zhong. The devil in linear transformer. *arXiv preprint arXiv:2210.10340*, 2022.

Zhen Qin, Songlin Yang, Weixuan Sun, Xuyang Shen, Dong Li, Weigao Sun, and Yiran Zhong. Hgrn2: Gated linear rnns with state expansion. *arXiv preprint arXiv:2404.07904*, 2024.

Hubert Ramsauer, Bernhard Schäfl, Johannes Lehner, Philipp Seidl, Michael Widrich, Thomas Adler, Lukas Gruber, Markus Holzleitner, Milena Pavlović, Geir Kjetil Sandve, et al. Hopfield networks is all you need. *arXiv preprint arXiv:2008.02217*, 2020.

Ruifeng Ren, Zhicong Li, and Yong Liu. Exploring the limitations of mamba in copy and cot reasoning. *arXiv preprint arXiv:2410.03810*, 2024.

Michael E Sander, Pierre Ablin, Mathieu Blondel, and Gabriel Peyré. Momentum residual neural networks. In *International Conference on Machine Learning*, pp. 9276–9287. PMLR, 2021.

Saul Santos, Vlad Niculae, Daniel McNamee, and Andre FT Martins. Sparse and structured hopfield networks. *arXiv preprint arXiv:2402.13725*, 2024.

Charlie Snell, Jaehoon Lee, Kelvin Xu, and Aviral Kumar. Scaling llm test-time compute optimally can be more effective than scaling model parameters. *arXiv preprint arXiv:2408.03314*, 2024.

Yu Sun, Xinhao Li, Karan Dalal, Jiarui Xu, Arjun Vikram, Genghan Zhang, Yann Dubois, Xinlei Chen, Xiaolong Wang, Sanmi Koyejo, et al. Learning to (learn at test time): Rnns with expressive hidden states. *arXiv preprint arXiv:2407.04620*, 2024.

Yutao Sun, Li Dong, Shaohan Huang, Shuming Ma, Yuqing Xia, Jilong Xue, Jianyong Wang, and Furu Wei. Retentive network: A successor to transformer for large language models. *arXiv preprint arXiv:2307.08621*, 2023.

Ilya Sutskever, James Martens, George Dahl, and Geoffrey Hinton. On the importance of initialization and momentum in deep learning. In *International conference on machine learning*, pp. 1139–1147. pmlr, 2013.

Yi Tay, Mostafa Dehghani, Dara Bahri, and Donald Metzler. Efficient transformers: A survey. 55 (6), December 2022. ISSN 0360-0300. doi: 10.1145/3530811. URL <https://doi.org/10.1145/3530811>.

Bahareh Tolooshams and Demba Ba. Stable and interpretable unrolled dictionary learning. *arXiv preprint arXiv:2106.00058*, 2021.

Constantino Tsallis. Possible generalization of boltzmann-gibbs statistics. *Journal of statistical physics*, 52(1):479–487, 1988.

Ashish Vaswani, Noam Shazeer, Niki Parmar, Jakob Uszkoreit, Llion Jones, Aidan N Gomez, Łukasz Kaiser, and Illia Polosukhin. Attention is all you need. *Advances in neural information processing systems*, 30, 2017.

Johannes von Oswald, Nino Scherrer, Seiji Kobayashi, Luca Versari, Songlin Yang, Maximilian Schlegel, Kaitlin Maile, Yanick Schimpf, Oliver Sieberling, Alexander Meulemans, et al. Mesanet: Sequence modeling by locally optimal test-time training. *arXiv preprint arXiv:2506.05233*, 2025.

Alex Wang, Amanpreet Singh, Julian Michael, Felix Hill, Omer Levy, and Samuel Bowman. Glue: A multi-task benchmark and analysis platform for natural language understanding. In *Proceedings of the 2018 EMNLP workshop BlackboxNLP: Analyzing and interpreting neural networks for NLP*, pp. 353–355, 2018.

Ke Alexander Wang, Jiaxin Shi, and Emily B Fox. Test-time regression: a unifying framework for designing sequence models with associative memory. *arXiv preprint arXiv:2501.12352*, 2025a.

Peng Wang, Yifu Lu, Yaodong Yu, Druv Pai, Qing Qu, and Yi Ma. Attention-only transformers via unrolled subspace denoising. *arXiv preprint arXiv:2506.03790*, 2025b.

Thomas Wolf, Lysandre Debut, Victor Sanh, Julien Chaumond, Clement Delangue, Anthony Moi, Pierrick Cistac, Tim Rault, Remi Louf, Morgan Funtowicz, et al. Transformers: State-of-the-art natural language processing. In *Proceedings of the 2020 conference on empirical methods in natural language processing: system demonstrations*, pp. 38–45, 2020.

Mitchell Wortsman, Peter J Liu, Lechao Xiao, Katie Everett, Alex Alemi, Ben Adlam, John D Co-Reyes, Izzeddin Gur, Abhishek Kumar, Roman Novak, et al. Small-scale proxies for large-scale transformer training instabilities, 2023. URL <https://arxiv.org/abs/2309.14322>.

Bohong Wu, Mengzhao Chen, Xiang Luo, Shen Yan, Qifan Yu, Fan Xia, Tianqi Zhang, Hongrui Zhan, Zheng Zhong, Xun Zhou, et al. Parallel loop transformer for efficient test-time computation scaling. *arXiv preprint arXiv:2510.24824*, 2025.

Dennis Wu, Jerry Yao-Chieh Hu, Weijian Li, Bo-Yu Chen, and Han Liu. Stanhop: Sparse tandem hopfield model for memory-enhanced time series prediction. *arXiv preprint arXiv:2312.17346*, 2023.

Dennis Wu, Jerry Yao-Chieh Hu, Teng-Yun Hsiao, and Han Liu. Uniform memory retrieval with larger capacity for modern hopfield models. *arXiv preprint arXiv:2404.03827*, 2024.

Liu Yang, Kangwook Lee, Robert Nowak, and Dimitris Papailiopoulos. Looped transformers are better at learning learning algorithms. *arXiv preprint arXiv:2311.12424*, 2023a.

Songlin Yang, Bailin Wang, Yikang Shen, Rameswar Panda, and Yoon Kim. Gated linear attention transformers with hardware-efficient training. *arXiv preprint arXiv:2312.06635*, 2023b.

Songlin Yang, Jan Kautz, and Ali Hatamizadeh. Gated delta networks: Improving mamba2 with delta rule. *arXiv preprint arXiv:2412.06464*, 2024.

Yongyi Yang, David P Wipf, et al. Transformers from an optimization perspective. *Advances in Neural Information Processing Systems*, 35:36958–36971, 2022.

Qifan Yu, Zhenyu He, Sijie Li, Xun Zhou, Jun Zhang, Jingjing Xu, and Di He. Enhancing autoregressive chain-of-thought through loop-aligned reasoning. *arXiv preprint arXiv:2502.08482*, 2025.

Yaodong Yu, Sam Buchanan, Druv Pai, Tianzhe Chu, Ziyang Wu, Shengbang Tong, Hao Bai, Yuexiang Zhai, Benjamin D Haeffele, and Yi Ma. White-box transformers via sparse rate reduction: Compression is all there is? *Journal of Machine Learning Research*, 25(300):1–128, 2024a.

Yaodong Yu, Sam Buchanan, Druv Pai, Tianzhe Chu, Ziyang Wu, Shengbang Tong, Benjamin Haeffele, and Yi Ma. White-box transformers via sparse rate reduction. *Advances in Neural Information Processing Systems*, 36, 2024b.

Qiyuan Zhang, Fuyuan Lyu, Zexu Sun, Lei Wang, Weixu Zhang, Wenyue Hua, Haolun Wu, Zhihan Guo, Yufei Wang, Niklas Muennighoff, et al. A survey on test-time scaling in large language models: What, how, where, and how well? *arXiv preprint arXiv:2503.24235*, 2025.

Daquan Zhou, Zhiding Yu, Enze Xie, Chaowei Xiao, Animashree Anandkumar, Jiashi Feng, and Jose M Alvarez. Understanding the robustness in vision transformers. In *International conference on machine learning*, pp. 27378–27394. PMLR, 2022.

Rui-Jie Zhu, Zixuan Wang, Kai Hua, Tianyu Zhang, Ziniu Li, Haoran Que, Boyi Wei, Zixin Wen, Fan Yin, He Xing, Lu Li, Jiajun Shi, Kaijing Ma, Shanda Li, Taylor Kergan, Andrew Smith, Xingwei Qu, Mude Hui, Bohong Wu, Qiyang Min, Hongzhi Huang, Xun Zhou, Wei Ye, Jiaheng Liu, Jian Yang, Yunfeng Shi, Chenghua Lin, Enduo Zhao, Tianle Cai, Ge Zhang, Wenhao Huang, Yoshua Bengio, and Jason Eshraghian. Scaling latent reasoning via looped language models. *arXiv preprint arXiv:2510.25741*, 2025.

A APPENDIX

A.1 MORE DISCUSSIONS ON LOOP TRANSFORMERS

In fact, by incorporating the global energy as a regularization term into the training objective, the model’s forward inference and backward propagation during training can be unified under the perspective of alternating optimization. As a classification example, we consider a single attention layer where the input is $\mathbf{H} = [\mathbf{h}_1, \dots, \mathbf{h}_N] \in \mathbb{R}^{d \times N}$ (e.g., embedded image patches)⁴ and \mathbf{z} serves as a special classification token (e.g., [CLS]) to compute the final representation. The model’s final output is typically projected via a projection head $\mathbf{E}^{d \times C}$ to obtain a logit matrix, which is then normalized by the softmax function and used to compute the cross-entropy loss, that is,

$$\text{CE}(\mathbf{E}^T \mathbf{z}, \mathbf{y}) = - \sum_{c=1}^C (\mathbf{y})_c \log \frac{e^{(\mathbf{E}^T \mathbf{z})_c}}{\sum_{u=1}^C e^{(\mathbf{E}^T \mathbf{z})_u}}, \quad (10)$$

where C denotes the number of classes, $\mathbf{y} \in \mathbb{R}^C$ is the (soft) label vector and $(\mathbf{y})_c$ denotes the probability of the c -th class. Then global energy F can be regarded as a regularization term on the cross-entropy loss: optimizing \mathbf{z} in the regularization corresponds to the forward computation, while optimizing the parameters corresponds to the backward propagation that updates the model. Formally, the overall objective can be written as

$$\min_{\mathbf{z}, \mathbf{W}, \mathbf{E}} \text{CE}(\mathbf{E}^T \mathbf{z}, \mathbf{y}) + F(\mathbf{z}, \mathbf{W}). \quad (11)$$

The process can be described by Algorithm 1, where we train the model with M samples for K epochs. Within each epoch, the forward inference and backward update can be viewed as an alternating optimization process over \mathbf{z} , \mathbf{W} and \mathbf{E} .

Algorithm 1 Unification via Alternating Optimization: One Single Attention Layer

Require: Training dataset of size M : $\{\mathbf{H}_i, \mathbf{y}_i\}_{i=1}^M$, learning rate η , training epochs K

Ensure: Updated parameters $\widehat{\mathbf{W}}$, $\widehat{\mathbf{E}}$ and representations $\{\widehat{\mathbf{z}}_i\}_{i=1}^M$

- 1: Initialize parameters $\mathbf{z}^0, \mathbf{E}^0, \mathbf{W}^0$
- 2: **for** each epoch $k = 0, \dots, K - 1$ **do** *# Train for K epochs with batch size M*
- 3: **for** each sample $i = 0, \dots, M - 1$ **do** *# Local GD on \mathbf{z} (equivalent to forward pass)*
- 4: $\mathbf{z}_i^{k+1} = \mathbf{z}_i^k - \eta \nabla_{\mathbf{z}} (\mathbf{z}_i^k, \mathbf{W}^k) = \text{Atten}(\mathbf{z}_i^k)$
- 5: **end for**
- 6: $\mathbf{W}^{k+1} = \mathbf{W}^k - \frac{\eta}{M} \sum_{i=1}^M \nabla_{\mathbf{W}} F(\mathbf{z}_i^{k+1}, \mathbf{W}^k)$ *# Local GD on \mathbf{W} (backpropagation)*
- 7: $\mathbf{E}^{k+1} = \mathbf{E}^k - \frac{\eta}{M} \nabla_{\mathbf{E}} \sum_{i=1}^M \text{CE}((\mathbf{E}^k)^T \mathbf{z}_i^{k+1}, \mathbf{y}_i)$ *# Local GD on \mathbf{E} (backpropagation)*
- 8: **end for**
- 9: Update $\widehat{\mathbf{W}} = \mathbf{W}^K$, $\widehat{\mathbf{E}} = \mathbf{E}^K$ and $\widehat{\mathbf{z}}_i = \mathbf{z}_i^K$ for $i = 1, \dots, M$
- 10: Return $\widehat{\mathbf{W}}, \widehat{\mathbf{E}}, \{\mathbf{z}_i^{(K)}\}_{i=1}^M$

While attention layers are commonly stacked with varying parameters across layers, Loop Transformers usually share parameters across iterations, helping preserve a relatively stable semantic space. In this case, the forward loop computation can be modeled as alternately updating $F(\mathbf{z}_i, \mathbf{H}, \mathbf{W})$ with respect to \mathbf{z}_i at each position, given the shared \mathbf{W} and the corresponding \mathbf{H} composed of attended set. Taking causal attention as an example, for the i -th position, the attended set typically consists of the preceding tokens $\mathbf{H}_{\leq i} = [\mathbf{h}_1, \dots, \mathbf{h}_i]$. Then the global objective is

$$\min_{\mathbf{Z}, \mathbf{H}} \sum_{i=1}^N F(\mathbf{z}_i, \mathbf{H}_{\leq i}, \mathbf{W}) \quad \text{s.t. } \mathbf{Z} = \mathbf{H}, \quad (12)$$

where $\mathbf{Z} = [\mathbf{z}_1, \dots, \mathbf{z}_N] \in \mathbb{R}^{d \times N}$. The constraint ensures that after each iteration, the tokens used in attended sets are aligned with the newly updated \mathbf{Z} . The iteration starts with the initialization $\mathbf{z}_i^0 = \mathbf{h}_i^0 = \mathbf{h}_i$. The forward computation of a single-layer Loop Transformer with K iterations can be equivalently viewed as performing K steps of gradient descent on each \mathbf{z} , which can be described by Algorithm 2

⁴To avoid introducing unnecessary new notation, here we omit the update of the embedding layer.

Algorithm 2 The Forward Inference of One-Layer Loop Transformer

Require: Learned \mathbf{W} , Tokens $\{\mathbf{h}_i\}_{i=1}^N$, temperature T , learning rate η
Ensure: Updated representation $\{\mathbf{z}_i^K\}_{i=1}^N$

- 1: Initialize $\mathbf{z}_i^0 = \mathbf{h}_i^0 = \mathbf{h}_i$ for $i = 1, \dots, N$
- 2: **for** each iteration $k = 0, \dots, K - 1$ **do** *# K iterations of Loop Transformer*
- 3: **for** each position $i = 1, \dots, N$ **do** *# Local GD on each \mathbf{z} (equivalent to forward pass)*
- 4: Update $\mathbf{z}_i^{k+1} = \mathbf{z}_i^k - \eta \nabla_{\mathbf{z}_i^k} F(\mathbf{z}_i^k, \mathbf{H}_{\leq i}; \mathbf{W}) = \text{Atten}(\mathbf{z}_i^k)$
- 5: **end for**
- 6: Update $\mathbf{h}_i^{k+1} = \mathbf{z}_i^{k+1}$ for $i = 1, \dots, N$
- 7: **end for**
- 8: Return $\{\mathbf{z}_i^K\}_{i=1}^N$

Unifying forward inference and backpropagation via alternating optimization. In fact, by incorporating Eq (12) as a regularization term into the training objective, the model's forward inference and backward propagation can be unified under the perspective of alternating optimization. For example, in autoregressive training, the model's final output representations \mathbf{Z} are typically projected onto the vocabulary to obtain a logit matrix, which is then normalized by the softmax function and used to compute the cross-entropy loss, that is,

$$\mathcal{L}(\mathbf{E}^T \mathbf{Z}, \mathbf{Y}) = - \sum_{i=1}^N \sum_{v=1}^V (\mathbf{y}_i)_v \log \frac{e^{(\mathbf{E}^T \mathbf{z}_i)_v}}{\sum_{u=1}^V e^{(\mathbf{E}^T \mathbf{z}_i)_u}}, \quad (13)$$

where V is the vocabulary size, $\mathbf{E} \in \mathbb{R}^{d \times V}$ is the final projection matrix and $\mathbf{Y} = [\mathbf{y}_1, \dots, \mathbf{y}_N] \in \mathbb{R}^{V \times N}$ is the label matrix often composed of N one-hot vectors. We also call $\mathbf{E}^T \mathbf{Z} \in \mathbb{R}^{V \times N}$ as the unnormalized logit matrix. Eq (12) can be regarded as a regularization term on the autoregressive loss: optimizing the representations \mathbf{Z} in the regularization corresponds to the forward computation, while optimizing the parameters corresponds to the backward propagation that updates the model. Formally, the overall objective can be written as

$$\min_{\mathbf{Z}, \mathbf{H}, \mathbf{W}, \mathbf{E}} \mathcal{L}(\mathbf{E}^T \mathbf{Z}, \mathbf{Y}) + \sum_{i=1}^N F(\mathbf{z}_i, \mathbf{H}_{\leq i}; \mathbf{W}), \quad s.t. \quad \mathbf{Z} = \mathbf{H}, \quad (14)$$

where \mathcal{L} is the cross-entropy loss as Eq 13. A single forward inference and backward update can be viewed as an alternating optimization process over \mathbf{Z} (or \mathbf{H}), \mathbf{W} , and \mathbf{E} , which can be described by Algorithm 3. In this way, the forward and backward processes can be unified as performing local GD on the regularized training loss, where the form of the regularization term is determined by the model architecture.

Algorithm 3 Unification via Alternating Optimization: One-Layer Loop Transformer

Require: Tokens $\{\mathbf{h}_i\}_{i=1}^N$, temperature T , learning rate η
Ensure: Updated representation $\{\mathbf{z}_i^K\}_{i=1}^N$, updated parameters $\widehat{\mathbf{W}}, \widehat{\mathbf{E}}$

- 1: Initialize parameters \mathbf{E}, \mathbf{W} and $\mathbf{z}_i^0 = \mathbf{h}_i^0 = \mathbf{h}_i$ for $i = 1, \dots, N$
- 2: **for** each iteration $k = 0, \dots, K - 1$ **do** *# K iterations of Loop Transformer*
- 3: **for** each position $i = 1, \dots, N$ **do** *# Local GD on \mathbf{z} (equivalent to forward pass)*
- 4: Update $\mathbf{z}_i^{k+1} = \mathbf{z}_i^k - \eta_k \nabla_{\mathbf{z}_i^k} F(\mathbf{z}_i^k, \mathbf{H}_{\leq i}^k; \mathbf{W}) = \text{Atten}(\mathbf{z}_i^k)$
- 5: **end for**
- 6: Update $\mathbf{h}_i^{k+1} = \mathbf{z}_i^{k+1}$ for $i = 1, \dots, N$
- 7: **end for**
- 8: Update $\widehat{\mathbf{W}} = \mathbf{W} - \eta \nabla_{\mathbf{W}} F(\mathbf{z}_i^k, \mathbf{H}_{\leq i}^k; \mathbf{W})$ *# Local GD on \mathbf{W} (backpropagation)*
- 9: Update $\widehat{\mathbf{E}} = \mathbf{E} - \eta \nabla_{\mathbf{E}} \mathcal{L}(\mathbf{E}^T \mathbf{Z}^K, \mathbf{Y})$ *# Local GD on \mathbf{E} (backpropagation)*
- 10: Return $\widehat{\mathbf{W}}, \widehat{\mathbf{E}}, \{\mathbf{z}_i^K\}_{i=1}^N$

A.2 PROOF OF LEMMA 1

Before presenting the proof of Lemma 1 for the multi-head case, we first provide the analysis for the single-head scenario as follows. We define $\tilde{F} = -T \log \sum_{i=1}^N e^{\frac{\mathbf{z}^T \mathbf{W} \mathbf{h}_i}{T}}$. When we relax the constraint for E_i in the softmax attention recipe so that $\|\mathbf{z}\| \leq \rho$ and $\|\mathbf{W} \mathbf{h}_i\| \leq \rho$ for all $i \in [N]$, we will have $F = -T \log \sum_{i=1}^N e^{-\frac{\|\mathbf{z} - \mathbf{W} \mathbf{h}_i\|^2}{2T}} \leq \tilde{F} + \rho^2$. For simplicity, we refer to \tilde{F} as the upper bound of F despite differing by a constant ρ^2 . Next we present the lemma for the single-head case.

Lemma 2 (Single-head Case). *Assuming $\|\mathbf{z}\| \leq \rho$ and $\|\mathbf{W} \mathbf{h}_i\| \leq \rho$ for all $i \in [N]$, both the global energy F and its upper bound \tilde{F} are non-convex with respect to \mathbf{z} . The local minima of F are attained at the boundary $\|\mathbf{z}\| = \rho$ or when $\mathbf{z} = \sum_{i=1}^N p_i \mathbf{W} \mathbf{h}_i$ where $p_i = \frac{1}{Z} e^{-\frac{\|\mathbf{z} - \mathbf{W} \mathbf{h}_i\|^2}{2T}}$ and $Z = \sum_{i=1}^N e^{-\frac{\|\mathbf{z} - \mathbf{W} \mathbf{h}_i\|^2}{2T}}$. In addition, the local minima of \tilde{F} are attained at the boundary $\|\mathbf{z}\| = \rho$.*

Proof. Recalling that in the single-head case $F = -T \log \sum_{i=1}^N e^{-\frac{\|\mathbf{z} - \mathbf{W} \mathbf{h}_i\|^2}{2T}}$. We can compute the derivative of F with respect to \mathbf{z} as

$$\nabla_{\mathbf{z}} F = -T \nabla_{\mathbf{z}} \log \sum_{i=1}^N e^{-\frac{\|\mathbf{z} - \mathbf{W} \mathbf{h}_i\|^2}{2T}} = \sum_{i=1}^N p_i (\mathbf{z} - \mathbf{W} \mathbf{h}_i),$$

where $p_i = \frac{1}{Z} e^{-\frac{\|\mathbf{z} - \mathbf{W} \mathbf{h}_i\|^2}{2T}}$ and $Z = \sum_{i=1}^N e^{-\frac{\|\mathbf{z} - \mathbf{W} \mathbf{h}_i\|^2}{2T}}$. For notational simplicity, we denote $\mathbf{r}_i = \mathbf{z} - \mathbf{W} \mathbf{h}_i$. To compute the Hessian matrix, we first calculate

$$\begin{aligned} \nabla_{\mathbf{z}} p_i &= \nabla_{\mathbf{z}} \frac{e^{-\frac{\|\mathbf{r}_i\|^2}{2T}}}{Z} = \frac{-\frac{1}{T} \mathbf{r}_i e^{-\frac{\|\mathbf{r}_i\|^2}{2T}} Z - e^{-\frac{\|\mathbf{r}_i\|^2}{2T}} \sum_{j=1}^N e^{-\frac{\|\mathbf{r}_j\|^2}{2T}} (-\frac{\mathbf{r}_j}{T})}{Z^2} \\ &= -\frac{1}{T} p_i \mathbf{r}_i + \frac{1}{T} p_i \sum_{j=1}^N p_j \mathbf{r}_j \end{aligned}$$

Therefore, the Hessian matrix of F with respect to \mathbf{z} is

$$\begin{aligned} \nabla_{\mathbf{z}}^2 F &= \sum_{i=1}^N \mathbf{r}_i \left(-\frac{1}{T} p_i \mathbf{r}_i^T + \frac{1}{T} p_i \sum_{j=1}^N p_j \mathbf{r}_j^T \right) + \mathbf{I} = \mathbf{I} - \frac{1}{T} \sum_{i=1}^N p_i \mathbf{r}_i \mathbf{r}_i^T + \frac{1}{T} \sum_{i=1}^N p_i \mathbf{r}_i \sum_{j=1}^N p_j \mathbf{r}_j^T \\ &= \mathbf{I} - \frac{1}{T} \left[\sum_{i=1}^N p_i \mathbf{r}_i \mathbf{r}_i^T - (\nabla_{\mathbf{z}} F) (\nabla_{\mathbf{z}} F)^T \right]. \end{aligned}$$

Furthermore, for any $\mathbf{v} \in \mathbb{R}^d$, we have

$$\mathbf{v}^T \nabla_{\mathbf{z}}^2 F \mathbf{v} = \|\mathbf{v}\|^2 - \frac{1}{T} \left[\sum_{i=1}^N p_i \mathbf{v}_i^T \mathbf{r}_i \mathbf{r}_i^T \mathbf{v}_i - (\mathbf{v}^T \nabla_{\mathbf{z}} F) (\mathbf{v}^T F)^T \right] \quad (15)$$

Let $X_i = \mathbf{r}_i^T \mathbf{v}$ and define a random variable X such that $P(X = X_i) = p_i$. Then for the second term in Eq (15), we have

$$-\frac{1}{T} \left[\sum_{i=1}^N p_i \|\mathbf{r}_i^T \mathbf{v}\|^2 - \left(\sum_{i=1}^N p_i \mathbf{r}_i^T \mathbf{v} \right)^2 \right] = -\frac{1}{T} [\mathbb{E}(X_i^2) - \mathbb{E}^2(X_i)] = -\frac{1}{T} \text{Var}(X) \leq 0.$$

Considering that the identity matrix is positive semi-definite, we obtain

$$\nabla_{\mathbf{z}}^2 F = \underbrace{\mathbf{I}}_{\succeq 0} - \underbrace{\frac{1}{T} \left[\sum_{i=1}^N p_i \mathbf{r}_i \mathbf{r}_i^T - (\nabla_{\mathbf{z}} F) (\nabla_{\mathbf{z}} F)^T \right]}_{\preceq 0}.$$

Therefore, we obtain that F is neither convex nor concave and when $\|\mathbf{z}\| \leq \rho$, its local minima can only be attained at the boundary $\|\mathbf{z}\| = \rho$ or at interior points where $\nabla_{\mathbf{z}} F = 0$, that is, $\mathbf{z} = \sum_{i=1}^N p_i \mathbf{W} \mathbf{h}_i$.

Similarly, we can obtain the Hessian matrix of \tilde{F} as

$$\nabla_{\mathbf{z}}^2 \tilde{F} = -\frac{1}{T} \left[\sum_{i=1}^N p_i (\mathbf{W} \mathbf{h}_i) (\mathbf{W} \mathbf{h}_i)^T - (\nabla_{\mathbf{z}} \tilde{F}) (\nabla_{\mathbf{z}} \tilde{F})^T \right] \preceq 0,$$

where $p_i = \frac{e^{\mathbf{z}^T \mathbf{W} \mathbf{h}_i / T}}{Z}$ and $Z = \sum_{i=1}^N e^{\frac{\mathbf{z}^T \mathbf{W} \mathbf{h}_i}{T}}$. Therefore, we can get that \tilde{F} is concave and when $\|\mathbf{z}\| \leq \rho$, its local minima can only be attained at the boundary $\|\mathbf{z}\| = \rho$. \square

We now present the proof of Lemma 1. In fact, noting that each head is independent, the proof is very similar to that of the single-head case. We define $\tilde{F} = -\frac{1}{H} \sum_{h=1}^H T \log \sum_{i=1}^N e^{-\mathbf{z}^T \mathbf{W}_{1,h}^T \mathbf{W}_{2,h} \mathbf{h}_i / T}$. Similarly, when we relax the constraint for $E_{h,i}$ in the recipe so that $\|\mathbf{W}_{1,h} \mathbf{z}\| \leq \rho$ and $\|\mathbf{W}_{2,h} \mathbf{h}_i\| \leq \rho$ for all $i \in [N]$ and $h \in [H]$, we will have $F \leq \tilde{F} + \rho^2$. For simplicity, we also refer to \tilde{F} as the upper bound of F despite differing by a constant ρ^2 . Next we present the lemma for the multi-head case.

Lemma 3. *Both the global energy F and its upper bound \tilde{F} are non-convex with respect to \mathbf{z} . Assuming $\|\mathbf{W}_{1,h} \mathbf{z}\| \leq \rho$ and $\|\mathbf{W}_{2,h} \mathbf{h}_i\| \leq \rho$ for all $i \in [N]$ and $h \in [H]$, the local minima of F are attained at the boundary $\|\mathbf{W}_{1,h} \mathbf{z}\| = \rho$ or when $\sum_{h=1}^H \sum_{i=1}^N p_{i,h} \mathbf{W}_{1,h}^T (\mathbf{W}_{1,h} \mathbf{z} - \mathbf{W}_{2,h} \mathbf{h}_i) = 0$ where $p_{i,h} = \frac{1}{Z_h} e^{-\|\mathbf{W}_{1,h} \mathbf{z} - \mathbf{W}_{2,h} \mathbf{h}_i\|^2 / 2T}$ and $Z_h = \sum_{i=1}^N e^{-\|\mathbf{W}_{1,h} \mathbf{z} - \mathbf{W}_{2,h} \mathbf{h}_i\|^2 / 2T}$. In addition, the local minima of \tilde{F} are attained when $\|\mathbf{W}_{1,h} \mathbf{z}\| = \rho$.*

Proof. Recalling that $F = -\frac{1}{H} \sum_{h=1}^H T \log \sum_{i=1}^N e^{-\frac{\|\mathbf{W}_{1,h} \mathbf{z} - \mathbf{W}_{2,h} \mathbf{h}_i\|^2}{2T}}$. We compute the derivative of F with respect to \mathbf{z} as

$$\nabla_{\mathbf{z}} F = \frac{1}{H} \sum_{h=1}^H \sum_{i=1}^N p_{i,h} \mathbf{W}_{1,h}^T (\mathbf{W}_{1,h} \mathbf{z} - \mathbf{W}_{2,h} \mathbf{h}_i),$$

where $p_{i,h} = \frac{1}{Z_h} e^{-\frac{\|\mathbf{W}_{1,h} \mathbf{z} - \mathbf{W}_{2,h} \mathbf{h}_i\|^2}{2T}}$ and $Z_h = \sum_{i=1}^N e^{-\frac{\|\mathbf{W}_{1,h} \mathbf{z} - \mathbf{W}_{2,h} \mathbf{h}_i\|^2}{2T}}$. Since the attention heads are independent of each other, the proof for each head is similar to that of Lemma 2. We denote $\mathbf{r}_{i,h} = \mathbf{W}_{1,h}^T (\mathbf{W}_{1,h} \mathbf{z} - \mathbf{W}_{2,h} \mathbf{h}_i)$ and to compute the Hessian matrix, we first calculate

$$\nabla_{\mathbf{z}} p_{i,h} = -\frac{1}{T} p_{i,h} \mathbf{r}_{i,h} + \frac{1}{T} p_{i,h} \sum_{j=1}^N p_{j,h} \mathbf{r}_{j,h}.$$

Then the Hessian matrix of F with respect to \mathbf{z} is

$$\begin{aligned} \nabla_{\mathbf{z}}^2 F &= \frac{1}{H} \sum_{h=1}^H \left[\sum_{i=1}^N \mathbf{r}_{i,h} \left(-\frac{1}{T} p_{i,h} \mathbf{r}_{i,h}^T + \frac{1}{T} p_{i,h} \sum_{j=1}^N p_{j,h} \mathbf{r}_{j,h}^T \right) + \mathbf{W}_{1,h}^T \mathbf{W}_{1,h} \right] \\ &= \frac{1}{H} \sum_{h=1}^H \underbrace{\left[\mathbf{W}_{1,h}^T \mathbf{W}_{1,h} - \frac{1}{T} \left(\sum_{i=1}^N p_{i,h} \mathbf{r}_{i,h} \mathbf{r}_{i,h}^T - (\nabla_{\mathbf{z}} F_h) (\nabla_{\mathbf{z}} F_h)^T \right) \right]}_{\succeq 0} \underbrace{\succeq 0}, \end{aligned}$$

where F_h^* is the Helmholtz free energy in the h -th subspace and $\nabla_{\mathbf{z}} F_h^* = \sum_{i=1}^N p_{i,h} \mathbf{r}_{i,h}$. Therefore, we obtain that F is neither convex nor concave and when $\|\mathbf{z}\| \leq \rho$, its local minima can only be attained at the boundary $\|\mathbf{z}\| = \rho$ or at interior points where $\nabla_{\mathbf{z}} F = 0$, that is, $\sum_{h=1}^H \sum_{i=1}^N p_{i,h} (\mathbf{W}_{1,h} \mathbf{z} - \mathbf{W}_{2,h} \mathbf{h}_i) = 0$. Similarly, we can obtain the Hessian matrix of \tilde{F} as

$$\nabla_{\mathbf{z}}^2 \tilde{F} = -\frac{1}{HT} \sum_{h=1}^H \left[\sum_{i=1}^N p_{i,h} \mathbf{r}_{i,h} \mathbf{r}_{i,h}^T - (\nabla_{\mathbf{z}} \tilde{F}_h) (\nabla_{\mathbf{z}} \tilde{F}_h)^T \right] \preceq 0,$$

where $p_{i,h} = \frac{e^{\mathbf{z}^T \mathbf{W}_{1,h}^T \mathbf{W}_{2,h} \mathbf{h}_i / T}}{Z_h}$ and $Z_h = \sum_{i=1}^N e^{\frac{\mathbf{z}^T \mathbf{W}_{1,h}^T \mathbf{W}_{2,h} \mathbf{h}_i}{T}}$. Therefore, we can get that \tilde{F} is concave and when $\|\mathbf{W}_{1,h} \mathbf{z}\| \leq \rho$, its local minima can only be attained at the boundary $\|\mathbf{W}_{1,h} \mathbf{z}\| = \rho$. \square

A.3 DETAILED DESIGN OF MHA2nd1st AND LightMHA2nd1st

A.3.1 MHA2nd1st

The update rule derived from the first-order gradient descent method for F is

$$\mathbf{z}^{(k+1)} = \mathbf{z}^{(k)} - \eta \nabla_{\mathbf{z}^{(k)}} F = \mathbf{z}^{(k)} - \frac{\eta}{H} \sum_{h=1}^H \sum_{i=1}^N p_{i,h} \mathbf{W}_{1,h}^T (\mathbf{W}_{1,h} \mathbf{z} - \mathbf{W}_{2,h} \mathbf{h}_i), \quad (16)$$

where $p_{i,h} = \frac{1}{Z_h} e^{-\frac{\|\mathbf{W}_{1,h} \mathbf{z} - \mathbf{W}_{2,h} \mathbf{h}_i\|^2}{2T}}$. The basic form using Newton's method based on second-order gradients is

$$\mathbf{z}^{(k+1)} = \mathbf{z}^{(k)} - \eta [\nabla_{\mathbf{z}^{(k)}}^2 F]^{-1} \nabla_{\mathbf{z}^{(k)}} F, \quad (17)$$

where $[\nabla_{\mathbf{z}^{(k)}}^2 F]^{-1}$ is the Hessian matrix at $\mathbf{z}^{(k)}$. We denote the Helmholtz free energy in the h -th subspace as $F_h = -T \log \sum_{i=1}^N Z_h$ and then $F = \frac{1}{H} \sum_{h=1}^H F_h$. Instead of applying Newton's method directly to F , we apply it independently to each subspace F_h , which can be formalized as

$$\mathbf{z}^{(k+1)} = \mathbf{z}^{(k)} - \frac{\eta}{H} \sum_{h=1}^H [\nabla_{\mathbf{z}^{(k)}}^2 F_h]^{-1} \nabla_{\mathbf{z}^{(k)}} F_h \quad (18)$$

Considering the analogous roles of $\mathbf{W}_{1,h}^T \mathbf{W}_{2,h}$ and $\mathbf{W}_{Q,h}^T \mathbf{W}_{K,h}$ in the recipe of multi-head softmax attention, we use the notation $\mathbf{q}_h = \mathbf{W}_{1,h} \mathbf{z}$, $\mathbf{k}_{i,h} = \mathbf{W}_{2,h} \mathbf{h}_i$ and $\bar{\mathbf{k}}_h = \sum_{i=1}^N p_{i,h} \mathbf{W}_{2,h} \mathbf{h}_i$. Then the Hessian matrix of F_h can be formulated as

$$\nabla_{\mathbf{z}}^2 F_h = \mathbf{W}_{1,h}^T \left[\mathbf{I} - \frac{1}{T} \sum_{i=1}^N p_{i,h} (\mathbf{k}_{i,h} - \bar{\mathbf{k}}_h) (\mathbf{k}_{i,h} - \bar{\mathbf{k}}_h)^T \right] \mathbf{W}_{1,h}. \quad (19)$$

Note that due to $\mathbf{W}_{1,h} \in \mathbb{R}^{\frac{d}{H} \times d}$, the Hessian matrix $\nabla_{\mathbf{z}}^2 F_h \in \mathbb{R}^{d \times d}$ is non-invertible. Therefore, we employ the range-space approach in Newton's method, i.e.,

$$[\nabla_{\mathbf{z}}^2 F_h]^{-1} = \mathbf{W}_{1,h}^T (\mathbf{W}_{1,h} \mathbf{W}_{1,h}^T)^{-1} \left[\mathbf{I} - \frac{1}{T} \sum_{i=1}^N p_{i,h} \mathbf{d}_{i,h} \mathbf{d}_{i,h}^T \right]^{-1} (\mathbf{W}_{1,h} \mathbf{W}_{1,h}^T)^{-1} \mathbf{W}_{1,h}, \quad (20)$$

where we use $\mathbf{d}_{i,h} = \mathbf{k}_{i,h} - \bar{\mathbf{k}}_h$ for simplicity. Furthermore, by parameterize $\mathbf{W}_{1,h}, \mathbf{W}_{2,h}$ as $\mathbf{W}_{Q,h}, \mathbf{W}_{K,h}$, the modification can be written as

$$\begin{aligned} \text{MHA2nd}(\mathbf{z}) &= \mathbf{z} + \frac{\eta}{H} \sum_{h=1}^H \mathbf{P}_h (\mathbf{q}_h - \bar{\mathbf{k}}_h), \\ \mathbf{P}_h &= \mathbf{W}_{Q,h}^T (\mathbf{W}_{Q,h} \mathbf{W}_{Q,h}^T)^{-1} \left[\mathbf{I} - \frac{1}{T} \sum_{i=1}^N p_{i,h} \mathbf{d}_{i,h} \mathbf{d}_{i,h}^T \right]^{-1}. \end{aligned} \quad (21)$$

Below, we first consider the computational cost for a single head. The cost to compute $\mathbf{q}_h - \bar{\mathbf{k}}_h$ and all $\mathbf{d}_{i,h}$ is $O(\frac{Nd}{H} + \frac{d^2}{H})$. It should be noted that $\mathbf{W}_{Q,h} \mathbf{W}_{Q,h}^T$ and its inverse only need to be pre-computed once and therefore the cost can be ignored when generating a large number of tokens. The cost of computing the outer products of N vectors and the inverse are $O(N \frac{d^2}{H^2} + \frac{d^3}{H^3})$. And performing the remaining matrix multiplications need $O(\frac{d^2}{H^2} + \frac{d^2}{H})$. Thus the total cost for one head is $O(N \frac{d^2}{H^2} + \frac{d^2}{H} + \frac{d^3}{H^3})$. Considering there are H heads, the final cost is $O(Nd \frac{d}{H} + d^2 + d^2 \frac{d}{H^2})$. Compared with $O(Nd + d^2)$ of standard attention, this incurs a higher computational cost.

To reduce the computational cost, we replace the matrix inversion with the first-order Taylor expansion, which can be formalized as

$$\begin{aligned} \text{MHA2nd1st}(\mathbf{z}) &= \mathbf{z} + \frac{\eta}{H} \sum_{h=1}^H \mathbf{P}_h (\mathbf{q}_h - \bar{\mathbf{k}}_h), \\ \mathbf{P}_h &= \mathbf{W}_{Q,h}^T (\mathbf{W}_{Q,h} \mathbf{W}_{Q,h}^T)^{-1} \left[\mathbf{I} + \frac{1}{T} \sum_{i=1}^N p_{i,h} \mathbf{d}_{i,h} \mathbf{d}_{i,h}^T \right]. \end{aligned} \quad (22)$$

In fact, this can be further simplified as

$$\begin{aligned} \text{MHA2nd1st}(\mathbf{z}) &= \mathbf{z} + \frac{\eta}{H} \sum_{h=1}^H \mathbf{M}_h (\mathbf{q}_h - \bar{\mathbf{k}}_h + \mathbf{b}_h), \\ \mathbf{M}_h &= \mathbf{W}_{Q,h}^T (\mathbf{W}_{Q,h} \mathbf{W}_{Q,h}^T)^{-1}, \quad \mathbf{b}_h = \frac{1}{T} \sum_{i=1}^N p_{i,h} \mathbf{d}_{i,h} [\mathbf{d}_{i,h}^T (\mathbf{q}_h - \bar{\mathbf{k}}_h)]. \end{aligned} \quad (23)$$

In this case, the cost to compute $\mathbf{q}_h - \bar{\mathbf{k}}_h$ and all $\mathbf{d}_{i,h}$ is still $O(\frac{Nd}{H} + \frac{d^2}{H})$. However, computing \mathbf{b}_h only needs $O(\frac{d^2}{H} + \frac{Nd}{H} + \frac{d^2}{H^2})$ by prioritizing the computation of inner products between vectors. Finally, the remaining cost of matrix multiplication is $O(\frac{d^2}{H})$. Therefore, the cost for each head is $O(\frac{Nd}{H} + \frac{d^2}{H})$ and the total cost for H heads is $O(Nd + d^2)$, which is of the same order as standard attention.

In practice, to avoid additionally computing and storing $\mathbf{d}_{i,h}$, we adopt the following form.

$$\begin{aligned} \text{MHA2nd1st}(\mathbf{z}) &= \mathbf{z} + \sum_{h=1}^H \mathbf{W}_{O,h} \mathbf{W}_{V,h} \mathbf{M}_h (\mathbf{q}_h - \bar{\mathbf{k}}_h + \mathbf{b}_h), \\ \mathbf{M}_h &= \mathbf{W}_{Q,h}^T (\mathbf{W}_{Q,h} \mathbf{W}_{Q,h}^T)^{-1}, \\ \mathbf{b}_h &= \frac{1}{T} \left[\sum_{i=1}^N p_{i,h} \mathbf{k}_{i,h} [\mathbf{k}_{i,h}^T (\mathbf{q}_h - \bar{\mathbf{k}}_h)] - \bar{\mathbf{k}}_h \bar{\mathbf{k}}_h^T (\mathbf{q}_h - \bar{\mathbf{k}}_h) \right]. \end{aligned} \quad (24)$$

Here we also introduce new parameters $\mathbf{W}_O \in \mathbb{R}^{d \times d_h}$, $\mathbf{W}_{V,h} \in \mathbb{R}^{d_h \times d}$ to make the model more flexible and the term $\frac{\eta}{H}$ is absorbed into these parameters. Moreover, to maintain stability, we set the temperature T in the attention score $p_{i,h}$ as a head-wise learnable parameter with initialization as $\sqrt{2d_h}$ and the temperature in \mathbf{b}_h is also learnable with initialization as 0.01.

A.3.2 LightMHA2nd1st

Since the form of MHA2nd1st appears somewhat cumbersome, we aim to design a more light variant that still preserves the core idea of utilizing second-order information for the update. One reason for the complexity of MHA2nd1st is that its energy function employs Euclidean distance-based attention. Therefore, we can instead shift our focus to the upper bound of F , that is, $\tilde{F} = -\frac{1}{H} \sum_{h=1}^H T \log \sum_{i=1}^N e^{\frac{\mathbf{z}^T \mathbf{W}_{1,h}^T \mathbf{W}_{2,h} \mathbf{h}_i}{T}}$, whose gradient is given by

$$\nabla_{\mathbf{z}} \tilde{F} = -\frac{1}{H} \sum_{h=1}^H \sum_{i=1}^N p_{i,h} \mathbf{W}_{1,h}^T \mathbf{W}_{2,h} \mathbf{h}_i,$$

where $p_{i,h} = \frac{e^{\frac{\mathbf{z}^T \mathbf{W}_{1,h}^T \mathbf{W}_{2,h} \mathbf{h}_i}{T}}}{Z_h}$. We can also get the Hessian matrix for the h -th head as

$$\nabla_{\mathbf{z}}^2 \tilde{F}_h = -\frac{1}{T} \mathbf{W}_{1,h}^T \mathbf{W}_{2,h} \left[\sum_{i=1}^N p_{i,h} (\mathbf{h}_i - \bar{\mathbf{h}}_h) (\mathbf{h}_i - \bar{\mathbf{h}}_h)^T \right] \mathbf{W}_{2,h}^T \mathbf{W}_{1,h},$$

where $\bar{\mathbf{h}}_h = \sum_{i=1}^N p_{i,h} \mathbf{h}_i$.

To make the formulation as concise as possible, we adopt the **parameterization-then-preconditioning** strategy. Specifically, considering the analogous roles of $\mathbf{W}_{1,h}^T \mathbf{W}_{2,h}$ and $\mathbf{W}_{Q,h}^T \mathbf{W}_{K,h}$, we first parameterize the $\mathbf{W}_{1,h}^T \mathbf{W}_{2,h}$ in the attention scores as $\mathbf{W}_{Q,h}^T \mathbf{W}_{K,h}$ meanwhile we use $\mathbf{W}_{V,h}$ to replace the remaining $\mathbf{W}_{1,h}^T \mathbf{W}_{2,h}$. Therefore, we have

$$\begin{aligned} \nabla_{\mathbf{z}} \tilde{F} &= -\frac{1}{H} \sum_{h=1}^H \sum_{i=1}^N p_{i,h} \mathbf{v}_{i,h} = -\frac{1}{H} \sum_{h=1}^H \bar{\mathbf{v}}_h, \\ \nabla_{\mathbf{z}}^2 \tilde{F}_h &= -\frac{1}{T} \left[\sum_{i=1}^N p_{i,h} (\mathbf{v}_{i,h} - \bar{\mathbf{v}}_h) (\mathbf{v}_{i,h} - \bar{\mathbf{v}}_h)^T \right], \end{aligned}$$

where $\mathbf{v}_{i,h} = \mathbf{W}_{V,h} \mathbf{h}_i$, $\bar{\mathbf{v}}_h = \sum_{i=1}^N p_{i,h} \mathbf{v}_{i,h}$ and $p_{i,h} = \frac{e^{\mathbf{z}^T \mathbf{w}_{\hat{Q},h}^T \mathbf{w}_{K,h} \mathbf{h}_i / T}}{Z_h}$. Then, we apply Newton’s Method independently to each subspace \tilde{F}_h to precondition the gradient, which can be formalized as

$$\mathbf{z}^{(k+1)} = \mathbf{z}^{(k)} - \frac{\eta}{H} \sum_{h=1}^H \left[\nabla_{\mathbf{z}^{(k)}}^2 \tilde{F}_h \right]^{-1} \nabla_{\mathbf{z}^{(k)}} \tilde{F}_h.$$

The corresponding attention can be formalized as

$$\text{LightMHA2nd}(\mathbf{z}) = \mathbf{z} - \frac{\eta}{HT} \sum_{h=1}^H \mathbf{W}_{O,h} \left[\epsilon \mathbf{I} + \sum_{i=1}^N p_{i,h} (\mathbf{v}_{i,h} - \bar{\mathbf{v}}_h) (\mathbf{v}_{i,h} - \bar{\mathbf{v}}_h)^T \right]^{-1} \bar{\mathbf{v}}_h,$$

where $\mathbf{W}_{O,h} \in \mathbb{R}^{d \times d_h}$ is introduced to keep the shape and we also use $\epsilon \mathbf{I}$ to facilitate the inversion of the Hessian matrix. Again, using the first-order Taylor expansion, we have

$$\text{LightMHA2nd1st}(\mathbf{z}) = \mathbf{z} - \frac{\eta \epsilon}{HT} \sum_{h=1}^H \mathbf{W}_{O,h} \left[\bar{\mathbf{v}}_h - \frac{1}{\epsilon} \sum_{i=1}^N p_{i,h} (\mathbf{v}_{i,h} - \bar{\mathbf{v}}_h) (\mathbf{v}_{i,h} - \bar{\mathbf{v}}_h)^T \bar{\mathbf{v}}_h \right].$$

Using $\sum_{i=1}^N p_{i,h} (\mathbf{v}_{i,h} - \bar{\mathbf{v}}_h) (\mathbf{v}_{i,h} - \bar{\mathbf{v}}_h)^T = \sum_{i=1}^N p_{i,h} \mathbf{v}_{i,h} \mathbf{v}_{i,h}^T - \bar{\mathbf{v}}_h \bar{\mathbf{v}}_h^T$, we have

$$\begin{aligned} \text{LightMHA2nd1st}(\mathbf{z}) &= \mathbf{z} + \sum_{h=1}^H \mathbf{W}_{O,h} (\bar{\mathbf{v}}_h + \tau_h \mathbf{b}_h), \\ \bar{\mathbf{v}}_h &= \sum_{i=1}^N p_{i,h} \mathbf{W}_{V,h} \mathbf{h}_i, \quad \mathbf{b}_h = \sum_i^N p_{i,h} \mathbf{v}_{i,h} \mathbf{v}_{i,h}^T \bar{\mathbf{v}}_h - \bar{\mathbf{v}}_h \bar{\mathbf{v}}_h^T \bar{\mathbf{v}}_h, \end{aligned}$$

where the term $-\frac{\eta \epsilon}{HT}$ is absorbed in $\mathbf{W}_{O,h}$ for simplify and we use τ_h are learnable parameters for each head with initialization as $\tau_h = 0.01$ to substitute $-\frac{1}{\epsilon}$. Similarly, we can prioritize the computation of vector–vector inner products in \mathbf{b}_h to avoid performing matrix–vector multiplications. The total cost is also $O(Nd + d^2)$; however, compared with standard softmax attention, it comes with a larger constant factor, though still smaller than that of MHA2nd1st.

A.4 MORE DETAILS OF EXPERIMENTS

To explore the potential of the proposed attention modifications, we conduct experiments using a GPT-like architecture(Brown et al., 2020). Specifically, we replace the original standard Softmax attention with the MomenMHA and NagMHA introduced in Section 3.1, as well as the MHA2nd1st and LightMHA2nd1st described in Section 3.2. For the FFN blocks, we use GELU (Hendrycks & Gimpel, 2016) as the activation function, and the hidden layer dimension is 4 times the input dimension. Considering our limited computational resources (two 24GB NVIDIA GeForce RTX 3090 GPUs), we conduct pre-training on the MiniPile dataset (Kaddour, 2023), which is a compact subset version of the original Pile dataset (Gao et al., 2020). We use the GPT-2 tokenizer from huggingface (Wolf et al., 2020) to process the corpus. We conduct training on the training set containing 1 million samples with the objective of next-token prediction with three epochs, while simultaneously monitoring and reporting the loss on the validation set. The model sizes range from 30M, 55M, and 76M to 160M parameters. These models have layers and attention heads in the ranges $\{6, 8, 8, 12\}$ and $\{4, 6, 8, 12\}$ respectively, with each head of dimensionality $d_h = 64$. For all models except the 160M one, we set the batch size to 32; for the 160M model, the batch size is set to 16. We use AdamW (Loshchilov, 2017) as the optimizer with a learning rate of lr = 1e - 4 with $\beta_1 = 0.9$, $\beta_2 = 0.999$, and employ a linear learning rate scheduler with warmup. We use a fixed dropout ratio of 0.1 for all experiments to improve generalization. For different tasks in the GLUE benchmark, we set the number of instruction fine-tuning epochs roughly according to the training set size: RTE and MRPC for 9 epochs, CoLA for 7 epochs, SST-2 for 5 epochs, and QNLI, QQP, and MNLI for 3 epochs.